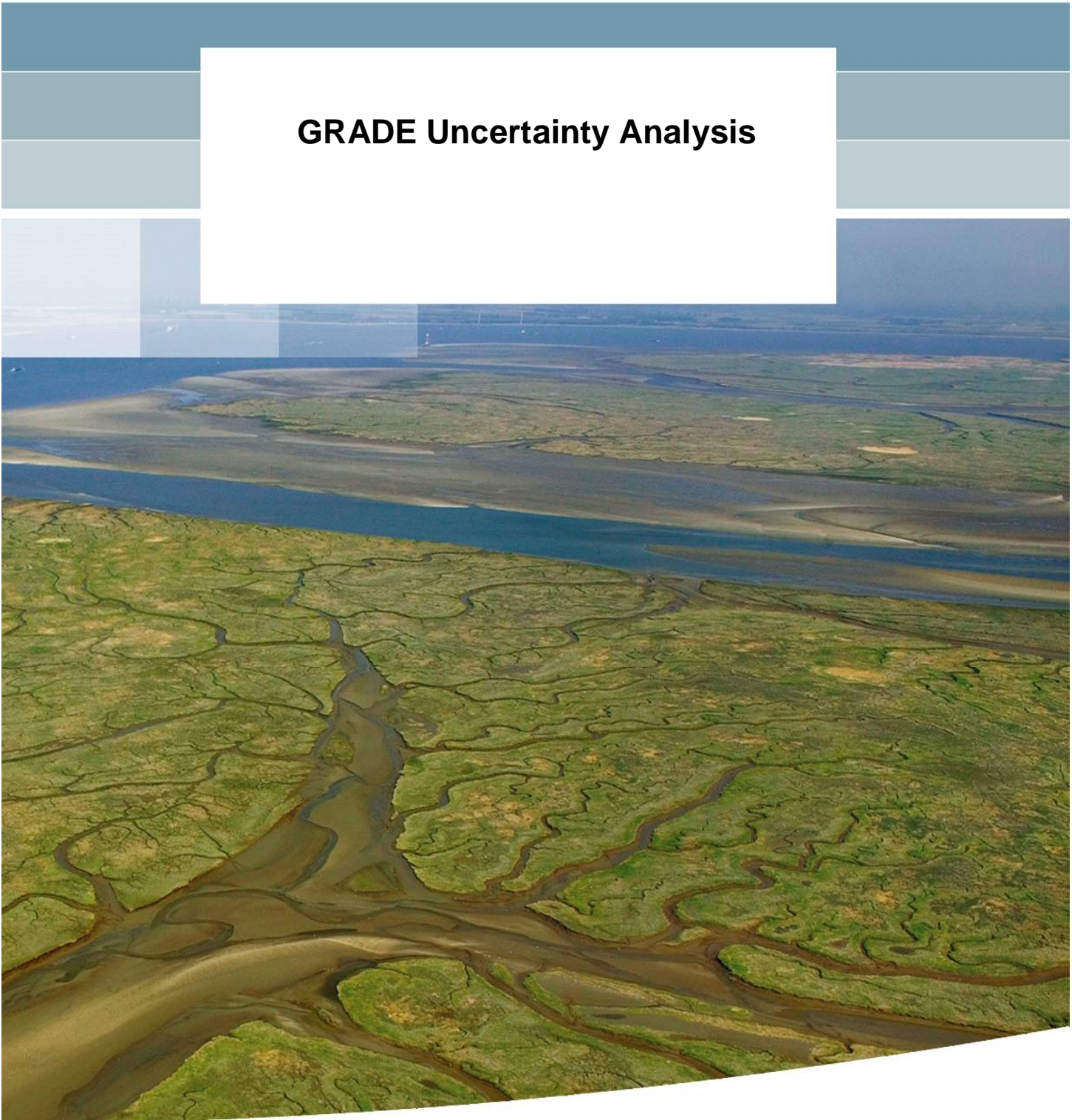


GRADE Uncertainty Analysis



GRADE Uncertainty Analysis

Henk van den Boogaard
Mark Hegnauer
Jules Beersma

1209424-004

Title
GRADE Uncertainty Analysis

Client	Project	Reference	Pages
Rijkswaterstaat WVL	1209424-004	1209424-004-ZWS-0003	65

Keywords

GRADE, Rhine, Meuse, extreme discharges, uncertainty analysis, frequency curves, synthetic weather series, hydrological and hydrodynamic models, flooding

Summary

A main purpose in a frequency or extreme value analysis is to obtain an estimate for some hydraulic or hydrologic quantity (e.g. a water level or a discharge at some location) that corresponds to a given return period. In traditional methods of frequency analysis observations are used. These are statistically extrapolated when estimates of extremes are desired for return periods much longer than the time period covered by the data. To overcome limitations in such traditional methods, GRADE (**G**enerator of **R**ainfall **A**nd **D**ischarge **E**xtrêmes) can be used as an alternative. In GRADE a chain of mathematical models is used for the generation of 'arbitrary' long term time series of discharges in a river system. Such GRADE systems are presently available for the rivers Rhine and Meuse.

The main issue addressed in this report is the derivation of the uncertainty that should be assigned to the estimates that GRADE produces for discharge extremes. These uncertainties in the by GRADE computed discharges are derived from uncertainties in GRADE's model components.

One of these components is formed by the temporally long term and spatially distributed weather (rainfall and temperature) series. The uncertainty in this component is here quantified by means of an ensemble of synthetically generated series of length 20,000 years. As a matter of the construction (using a stochastic weather generator) the variability in this ensemble reflects the current climate uncertainty.

The hydrological HBV models form a second source of uncertainty in the GRADE system. The uncertainty in these hydrological models is also quantified by means of an ensemble. This ensemble consists of five sets of HBV model parameter-combinations, which reflect the model parameter uncertainty of the HBV model.

Uncertainties in the hydrodynamic SOBEK models that are used for the routing of (extreme) flows along the main river channel are a third source of uncertainty. In the present work these uncertainties are not yet taken into account, however.

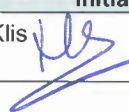
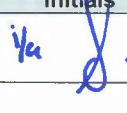

For every combination of the synthetic weather series and a set of HBV-parameters a GRADE simulation of 20,000 years is carried out. In the report below it is described how the results of these GRADE computations are combined to obtain the uncertainty in the estimates of the extreme discharges.

Title
GRADE Uncertainty Analysis

Client Rijkswaterstaat WVL **Project** 1209424-004 **Reference** 1209424-004-ZWS-0003 **Pages** 65

This uncertainty analysis has been applied to derive the uncertainties in the GRADE estimates of extreme discharges of the Rhine at Lobith and the Meuse at Borgharen. The results are illustrated by means of discharge frequency curves for return periods up to 50,000 year. It is also verified to what extent the (uncertainties in) the various model components in GRADE contribute to the total uncertainty in the discharges. Moreover for the Rhine the effects of taking upstream flooding into account are established. On the basis of SOBEK-models with and without flooding it is found that flooding significantly reduces the Lobith discharges for return periods longer than about 50 year. For example, for a return period of 10,000 year this reduction amounts about 4000 m³/s. At the same time the width of the confidence bands is also (and even much more substantially) reduced.

In a separate variational (rather than uncertainty) analysis the sensitivity of extreme Lobith discharges on uncertain parameters in the upstream flooding mechanisms is examined.

Version	Date	Author	Initials	Review	Initials	Approval	Initials
	July 2014	H.F.P. van den Boogaard		H. van der Klis		G. Blom	
		M. Hegnauer					
		J.J. Beersma					

State
Final

Contents

1 Introduction	1
1.1 Background of GRADE	1
1.2 Uncertainty analysis GRADE	3
2 Description of the uncertainties in the GRADE components	5
2.1 Uncertainties in the stochastic weather generators for the Meuse and Rhine basins	5
2.2 Uncertainties in the HBV rainfall-runoff models	7
2.3 Uncertainties in the hydrodynamic SOBEK models	10
3 Method of the GRADE uncertainty analysis	13
3.1 The uncertainty matrix	13
3.2 Computation of the uncertainty matrix	14
3.3 Variance reduction using Weissman's method	14
3.4 Quantifying the uncertainties in the climate	14
3.5 Quantifying the uncertainties in the hydrological models	14
3.6 Combination of the uncertainties in the climate and the hydrological models	15
4 GRADE uncertainty analysis for discharge extremes for the Rhine at Lobith	17
4.1 HBV estimates and uncertainties of extreme discharges at Lobith	17
4.2 SOBEK estimates and uncertainties of extreme Lobith discharges (without flooding)	23
4.3 SOBEK estimates and uncertainties of extreme Lobith discharges (with flooding)	26
4.4 Sensitivity analysis of flooding parameters in the SOBEK model	29
5 GRADE uncertainty analysis for discharge extremes for the Meuse at Borgharen	33
6 Final GRADE discharge frequency curves and uncertainties for Lobith and Borgharen	39
7 Summary and conclusions	43
7.1 Summary	43
7.2 Conclusions	44
8 Remarks, discussion and further developments	45
9 Literature	47

Appendices

A Description of the GRADE uncertainty analysis method	49
A.1 The uncertainty matrix	49
A.2 Computation of the uncertainty matrix	50
A.3 Variance reduction using Weissman's method	51
A.4 Quantifying the uncertainties in the climate	53
A.5 Quantifying the uncertainties in the hydrological models	55
A.6 Combination of the uncertainties in the climate and hydrological models	58
B Regression of HBV and SOBEK estimates of extreme Rhine discharges at Lobith	61
B.1 SOBEK without flooding	61
B.2 SOBEK with flooding	62
B.3 Comparison of HBV and SOBEK \pm Flooding	63
C Regression of HBV and SOBEK estimates of extreme discharges of the Meuse at Borgharen	65

1 Introduction

1.1 Background of GRADE

A main purpose in a frequency or extreme value analysis is to obtain an estimate for some hydraulic or hydrologic quantity (as for example a water level or a discharge at one or more locations in a water system) that corresponds to a given probability of exceedence or some return period.

Traditionally observed extreme values of the 'target' variable are used in frequency analysis. The common procedure is to select the annual extremes of an observed time series, or peak values that exceed some (sufficiently high) threshold. This sample of extreme values is then used to identify the parameters of a probability distribution that provides a statistical model for the selected extreme values. From this fitted distribution estimates of the target variable can be derived for any desired return period and particular for return periods that may be much longer than the length of the observed data record. In that case the identified distribution is actually used for statistical extrapolation.

This method of frequency analysis is quite generic and straightforward to apply. On the other hand several limitations can be present. For example, the sample of selected extreme values should be sufficiently large to obtain accurate estimates for the parameters in the probability distribution. Also the results of the frequency analysis may depend heavily on the chosen probability distribution. At the same time estimates for larger return periods than the observation time length are only meaningful if the observed data (or actually the underlying physical system) represent a stationary and/or homogeneous physical process. For other and a more detailed inventory and discussion of such limitations of the traditional method of frequency analysis one is referred to e.g. Ogink (2012).

Until now, this traditional frequency analysis was also used for the estimation of extremely high discharges of the Rhine at Lobith, and the Meuse at Borgharen. To overcome many of the limitations of the frequency analysis an alternative method called GRADE has been developed in joint cooperation by Rijkswaterstaat Water, Verkeer en Leefomgeving (WVL), Royal Netherlands Meteorological Institute (KNMI), and Deltares. GRADE stands for **Generator of Rainfall And Discharge Extremes**. In GRADE a chain of mathematical models is used for the generation of 'arbitrary' long term time series of discharges in a river system. Rather than observed values the so generated time series are used in a frequency analysis. At the moment such GRADE-models have been developed for the Meuse and the Rhine system. In this modelling all contributing (sub-)basins and/or tributaries of each river system and their (geophysical) characteristics relevant for the genesis of extreme flows in the main river are in large detail taken into account.

The "architecture" of GRADE systems for the Meuse and Rhine is graphically illustrated in Figure 1.1. In this figure three main (model) components can be recognised.

The first component ("Stochastic weather generator") is a stochastic rainfall and temperature generator. With this component spatially distributed (covering all relevant catchment areas of the river basin) and temporally arbitrary long series of daily precipitation and temperature can be produced. The core of this weather generator is a nearest neighbour resampling of historic observed (and also spatially distributed) weather variables. As a matter of the procedure statistical properties (as for example mutual correlations of the simulated variables) of so generated synthetic weather data are preserved compared to the historic data.

For detailed information on this generation of long synthetic rainfall/temperature series one is referred to Buishand and Brandsma (2001), Leander et al. (2005), Buishand and Leander (2011), and Schmeits et al. (2014a, b).

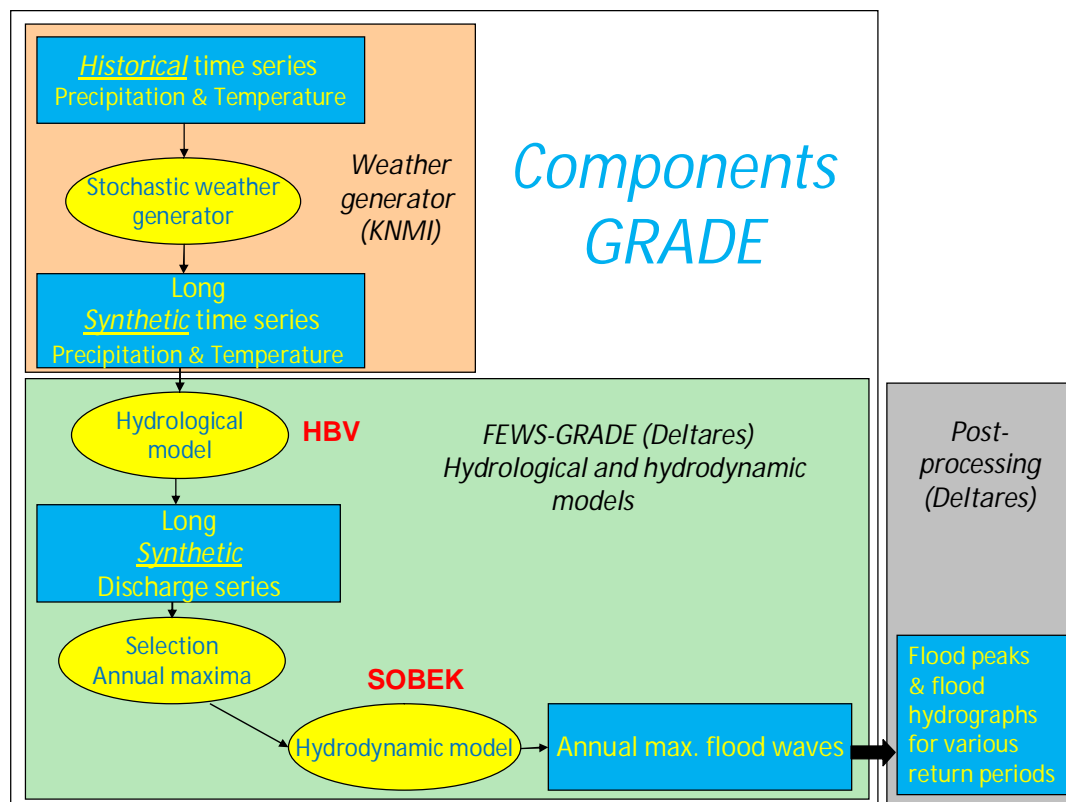


Figure 1.1 Architecture of the GRADE systems for the Meuse and Rhine

The second component in the GRADE system (“Hydrological model”) consists of hydrological models to simulate the precipitation-runoff processes in the various (sub) basins of the river system. For both the Meuse and the Rhine the HBV model developed by the SMHI (Sweden) is used for this purpose. The HBV-model is a lumped-distributed or semi distributed conceptual model with a large number of parameters in the formulation of the several rainfall-runoff sub-processes. A main activity in the preparation of the present GRADE systems was the calibration of the HBV models for the various sub-basins. See Winsemius et al. (2013), Hegnauer and Van Verseveld (2013); Kramer et al. (2008). In this calibration measured data of rainfall and runoff is used. In GRADE computations, however, the synthetic weather variables described above serve as input for the thus calibrated hydrological models.

The third component in the GRADE-systems (“Hydrodynamic model”) involves the simulation of the (propagation of) most extreme flows along the main river system with a hydrodynamic model. In general the 1D flow model SOBEK is used for this simulation. But also in the HBV-models flow routing facilities are present. However, the HBV-schematization of this routing is rather “rough” and may not sufficiently accurately represent the river and flood plain characteristics (such as plain dimensions, roughness, conveyance limits, etc.) that affect the propagation and attenuation of flood waves. These effects are particular relevant for extreme floods and in that case the SOBEK results are expected to provide better estimates than those produced by HBV.

As a matter of its set up the GRADE system has important advantages compared to the traditional method of frequency analysis. In fact:

- By means of the conceptual hydrological and hydraulic models the system has a sound physical basis.
- In this way, and in contrast to the traditional method, GRADE can also deal with the effects of overflows, inundations, conveyance limitations, etc., that may turn up for very high flows. In these circumstances GRADE based estimates of (very) extreme flows will be much more accurate than those found by statistical extrapolation of measurements.
- The data record with extreme values can be made arbitrarily long.
- It is possible to simulate the effect of changes/interventions in the flow area, and/or climate changes.
- Estimates for extreme values for prescribed return periods (and/or return level plots) can be generated for virtually any location in the river system and are not restricted to monitoring positions.

1.2 Uncertainty analysis GRADE

The main issue in this report is an uncertainty estimation of the extreme discharges computed by GRADE. The ultimate goal is the derivation of discharge frequency curves for the river Rhine at Lobith and the river Meuse at Borgharen, together with the 95% confidence bands for these discharges. In *frequency* curves peak discharges are plotted or tabulated versus the corresponding return period (for this reason frequency curves are sometimes also called *return level plots*).

In this uncertainty analysis the amount that the various sources of uncertainty within GRADE contribute to the total uncertainty is considered in particular. In this case these sources of uncertainty refer to two model components of GRADE: the weather climate (rainfall and temperature series providing the input for the hydrological models) and the hydrological models (HBV). Presently, uncertainties in a third important component, the hydrodynamic model (SOBEK) used for the propagation of the flood along the main river, are not taken into account.

For the river Rhine the uncertainty analysis is carried in twofold. In one case using a SOBEK version in which upstream flooding is not modeled, and in the other case a SOBEK model in which flooding is also taken into account. In this way the effect of flooding on the frequency curves and associated uncertainty can quantitatively be established. In advance it is mentioned that the effects of flooding (on both the discharges and their uncertainty) turn out to be large.

As already mentioned uncertainties in the hydrodynamic SOBEK models have not been taken into account. Instead results of a sensitivity analysis will be presented for the SOBEK model with flooding for the Rhine. These results indicate that uncertainties in the modeling of flooding may also have non-negligible effects on the total uncertainty in the Lobith frequency curve.

The remainder of this report is organized as follows. Chapter 2 provides a description of the uncertainties of the individual model components of GRADE. Chapter 3 deals with the procedure for the combination of these uncertainties. In Chapter 4 the results of the uncertainty analysis can be found for the Rhine at Lobith, and in Chapter 5 for the Meuse at Borgharen.

Within the present scope (with GRADE brought into the WTI¹ project) estimates and uncertainties for extreme discharges at Lobith and Borgharen are desired for return periods up to 100,000 years. Because of computation time the GRADE simulations in the uncertainty analysis were limited to a length of 20,000 years, however. The so called Weissman method is used to determine the uncertainties in the frequency curves for return periods between 250 and 100,000 years. These 'final' results for the discharge frequency curves are shown in Chapter 6.

In Chapter 7 the main results and conclusions of the present study are summarized while further remarks and discussion are finally presented in Chapter 8.

¹ WTI stands for "Wettelijk Toets Instrumentarium". WTI is the Dutch method for analyzing dikes along the Dutch primary and secondary flood defense structures.

2 Description of the uncertainties in the GRADE components

2.1 Uncertainties in the stochastic weather generators for the Meuse and Rhine basins

In this section the main aspects of the representation of uncertainties in the rainfall and temperature series generated by the stochastic weather generator are described.

Section summary

The uncertainty in the first component of the GRADE system for the Meuse and the Rhine is made available through a set of *synthetically* generated weather time series.

Within the uncertainty analysis these series will all be of length 20,000 *years*. However, in the estimation of the 'final' return levels for extreme discharges up to return periods of 10,000 years at Lobith (Rhine) and Borgharen (Meuse), the "reference" 50,000 *years* synthetic weather series and corresponding GRADE simulations have been used.

As a matter of the construction of the synthetic rainfall and temperature series each of these series represents a "possible" realization of the weather variables according to the *present* weather climate. The variability in the various realizations thus reflects the current climate uncertainty.

The set of these synthetic weather series can be considered as a "discrete" or "empirical" probability distribution for the uncertainty in the precipitation and temperature, expressed as the uncertainty in weather series simulated with the weather generator. Within GRADE this uncertainty represents the uncertainty in the input for the rainfall-runoff models.

For the Rhine basin a set of 11 of such synthetic rainfall and temperature series is constructed, compared to a set of 24 series for the Meuse.

Estimates of (extreme) discharges at Borgharen and/or Lobith (and in the event at other locations along the rivers) are needed for return periods much longer than the time period for which measurements are available. Therefore very long synthetic rainfall and temperature series are used, rather than short measurement series. The synthetic rainfall and temperature series are generated by means of a stochastic weather generator which uses a resampling procedure of available historic (observed) rainfall and temperature data. In this way arbitrary long time series of rainfall and temperature can be generated, and consequently also long enough with respect to the return periods which are required. An important characteristic of the method is that the statistical properties of the long synthetic series are consistent with those of the historic data on which the synthetic series are based. For a more detailed description of the background and construction of long synthetic rainfall and temperature series and the associated uncertainties one is referred to Buishand and Brandsma (2001), Leander et al. (2005), Buishand and Leander (2011), and Schmeits et al. (2014a,b).

In first instance all available historic weather data can be used as the basis set for the generation of a long synthetic time series of the weather variables. This would provide merely one realization of a long synthetic series. A main source of uncertainty is the *representativeness* of this basis set and the subsequent synthetic series. To quantify the effect of this uncertainty on the resulting statistics of extreme discharges a resampling method is followed. See Efron and Tibshirani (1993) for an introduction to resampling techniques and the way such techniques can be used for the estimation of uncertainties in a statistic derived from a data set.

In resampling (not to be confused with the nearest neighbor resampling mentioned above that is used within the stochastic weather generator) an ensemble of replicates is constructed of an 'original' observed data set. Each replicate is a subset of the original data set (actually a sample taken from the original set to which an empirical probability distribution is assigned; for this reason the replicate is usually called a resample). In the present case resamples are constructed from the observed rainfall and temperature data set. Each resample serves as a 'new' basis set for the weather generator and for each resample a separate long synthetic series is constructed. In the end this gives an ensemble of long synthetic rainfall and temperature series. In GRADE these series serve as input for the rainfall-runoff models and in this way climate uncertainty is imported in the modeling.

In the presently applied resampling a Jackknife procedure is followed for the construction of an ensemble of basis sets. In this case blocks of consecutive observations are deleted. For the Meuse basin these blocks are chosen of length three years. With an available data record of length 72 years (within the time period 1930-2008), this leads to 24 resampled basis sets for the weather generator, resulting in an ensemble of 24 generated synthetic weather data sets for the uncertainty analysis of GRADE. In a similar way 11 long synthetic rainfall data sets were derived for the Rhine basin (55 years of historic weather data and a block length of five years in the Jackknife resampling). In the choice of the block length and/or ensemble size a balance had to be found between accuracy in the representation of uncertainties in the weather climate (promoting a block length as small as possible and an ensemble size as large as possible) and the associated computational burden (ensemble size as small as possible).

As already mentioned, estimates and uncertainties for extreme discharges at Lobith (Rhine) and Borgharen (Meuse) are desired for return periods up to 10,000 years. Therefore the length of the synthetic weather series should preferably be of this length (or even longer) as well. The reference GRADE simulations consist of 50,000 years simulations for both the Meuse and the Rhine. However, for the uncertainty analysis the length of the GRADE simulations was limited to 20,000 years, due to the extensive computing time.

The "reference" GRADE simulations correspond to the case with the reference weather generator series (which are based on the full set of historical precipitation and temperature data), combined with the reference parameter set for the hydrological models (see Section 2.2). To improve the uncertainty estimates for the highest extremes (with return periods between 250 and 100,000 years), use is made of Weissman's method (Weissman, 1978). This method is described in Section A.3 of Appendix A.

2.2 Uncertainties in the HBV rainfall-runoff models

This section describes the origin and construction of the HBV parameter combinations.

Section summary

For both the Rhine and Meuse the uncertainty in the hydrological models is represented by five different combinations of HBV-model parameters.

In preceding work these five combinations were derived within a joint *calibration* and *uncertainty analysis* of the HBV models for the various sub-basins.

Due to the way these five combinations were selected (from a much larger set of parameter combinations that satisfy the calibration criteria) they are not equally likely. In the uncertainty analysis a different weight is therefore assigned to each of these five combinations. In the end the five parameter combinations and their weight are then used as an (“empirical”) probability distribution for the total uncertainty in the hydrological models.

An important activity in the set-up of the GRADE system was the calibration of the HBV rainfall-runoff models for the various river (sub-) basins. In this calibration observed data of the model’s input and output (such as rainfall, temperature, and discharges) was used to derive estimates for a selected set of uncertain parameters in the HBV-models. Three criteria were defined to quantify the quality of the models for reproducing the observed data and to determine for which setting(s) of the parameters the best performance is found. A detailed description of the set up and the results of the calibration of the HBV-models in the GRADE systems for the Meuse can be found in Kramer et al. (2008). For the Rhine basins one is referred to Winsemius et al. (2013) and Hegnauer and Van Verseveld (2013).

In the calibration of the HBV models a Generalized Uncertainty Estimation method (GLUE, see Beven and Binley, 1992) was used. In this way the calibration of the models is actually combined with an uncertainty assessment. As a result the final outcome of the calibration of an HBV-model for a particular basin consists of a set of “behavioral” parameter combinations rather than a single ‘deterministic’ estimate for the uncertain model parameters. A parameter combination is called “behavioral” if the resulting model response satisfies the calibration criteria. Elsewhere in this report (Section A.5 in Appendix A) it is described how to each parameter combination a probability is assigned. At that moment the set of parameter combinations can be considered as an empirical probability distribution for the parameters, and as such a representation of the uncertainty in the parameters and thus in the HBV-models. Apart from these parameters no other uncertainties were taken into account in the HBV-models.

For a given state of the climate (represented by a member from the Weather Generator set) the uncertainties in the output of the HBV-models are thus determined by the uncertainties in the model parameters. Due to the complexity of the HBV-models the uncertainty in their response cannot be obtained in analytical form. To obtain quantitative estimates for the model predictions one cannot do much better than to evaluate the model for all (or a subset, see below) behavioral parameter combinations and in this way (again) produce an empirical distribution of the output. From this distribution additional measures for the representation of the uncertainty in the output can be derived such as a mean, spread, quantiles, or a confidence interval.

For individual (sub-) basins of the Rhine or Meuse the number of behavioral parameter combinations varied from about ten to several hundred. For the river basin as a whole, parameters from the individual sub-basins is combined to obtain a single parameter combination. For the Meuse 15 of such sub-basins are discriminated within the hydrological modeling, while for the Rhine in total 148 sub-basins are defined for the 15 major sub-basins. See Figure 2.2.1 (Meuse) and Figure 2.2.2 (Rhine).

Due to the large number of sub-basins the total number of behavioral combinations for the whole river basin (especially for the Rhine) becomes extremely large. In fact, much too large to allow an uncertainty assessment where the model is evaluated for all possible combinations of the behavioral parameter combinations of the sub-basins.

Therefore the number of parameter combinations for which in an uncertainty analysis the model is evaluated must be substantially reduced. This in particular is the case in an uncertainty analysis where 20,000 years long synthetic series are used.

Selection procedures have been applied to reduce the number of behavioral parameter combinations for the Rhine to form a representative and for computationally manageable subset. In the end for each major sub-basin of the Rhine the number of behavioral parameter combinations for that sub-basin was reduced to five. This was done in a way that these selected combinations reasonably cover the uncertainty range of the HBV model in predicting extremes and thus provide a representative subset. See Winsemius et al. (2013) for further details.

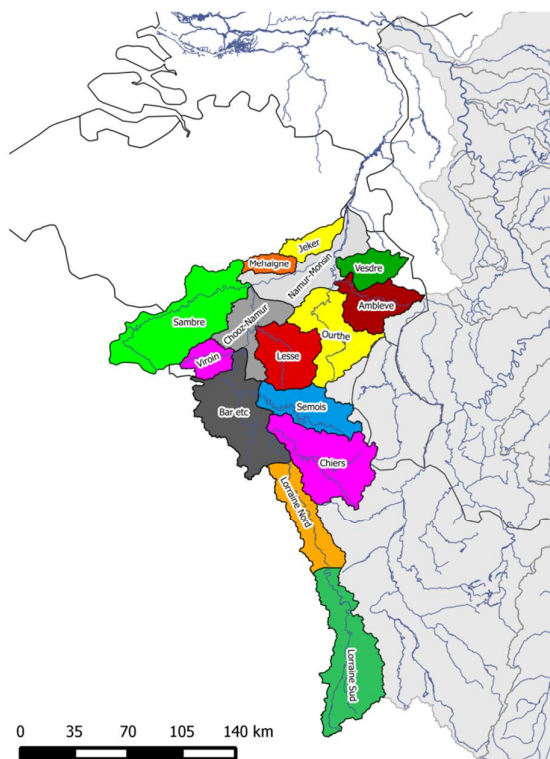


Figure 2.2.1 Sub-basins (15) in the hydrological modelling of the Meuse

The period for which the model's calibration took place is 1985-2006. For each parameter set the annual maxima were derived and subjected to an empirical frequency analysis. For a return period of 10 years the corresponding discharge extreme (at a sub-basin's downstream location) was selected. From the empirical distribution of these 'extreme' discharges (as many as the number of behavioral HBV-parameter combinations) the 5%, 25%, 50%, 75%, and 95% quantiles were determined and the corresponding HBV parameter combination selected.

To investigate the sensitivity for the chosen return period, also for the discharges of the 2 and 5 year return period selection procedure was performed. However, it was found that the return period had no significant influence on the selected parameter sets and thus the return period of 10 years was used in the remainder. For a more complete description of this selection procedure one is referred to Winsemius et al. (2013), and Hegnauer and Van Verseveld (2013).

Finally five representative parameter combinations are constructed for each major sub-basin. For the whole Rhine basin, consisting of 15 major sub-basins, combinations of these representative parameter sets should be made. This would result in 5^{15} possible parameter combinations for the whole Rhine basin. This number of possibilities is still much too large and a further reduction is needed. This further reduction is achieved by "quantile-wise combination" of the parameter sets of the sub-basins. Effectively this means that for the 5%-parameter combination for the whole Rhine basin the 5%-parameter sets from all 15 major sub-basins are used. The same procedure is followed for the 25%-, 50%-, 75%- and 95%-parameter combinations.

With this procedure it is implicitly assumed that the parameter combinations of the major sub-basins are fully (or at least to a high extent) dependent. This assumption is not unreasonable as in the calibration/GLUE procedure the selection of behavioral combinations was first done for the upstream HBV sub-basins. Subsequently the results for these upstream basins were used in the construction and selection of the behavioral parameter combinations of next downstream sub-basins.

For the Meuse a slightly different approach was followed to select and reduce the number of behavioral parameter combinations to five. In this case the selection is based on the simulated once in 100 year discharges at Borgharen. These were determined for a subset of 500 (out of 2949) behavioral HBV-parameter combinations for the Meuse sub-basin upstream of Liège. In this case simulations of length 3000 years were carried out with synthetically generated rainfall and temperature series. From the distribution of the Borgharen discharges for the 100 year return period, the 5, 25, 50, 75, and 95% quantiles were again determined and the corresponding HBV-parameter combinations selected. For further details see Kramer et al. (2008) and Ogink (2012).

2.3 Uncertainties in the hydrodynamic SOBEK models

In this section, the uncertainties in the hydrodynamic models are discussed.

Section summary

In the present uncertainty analysis no extensive uncertainty analysis was performed for hydrodynamic SOBEK models.

Instead, for the Rhine a comparison is made of frequency curves with and without flooding taken into account.

For the SOBEK model with flooding, a basic sensitivity (rather than uncertainty) analysis is presented to get an impression of the effects of – and sensitivities for – uncertain parameters in the modeling of flooding mechanisms.

SOBEK is used as hydrodynamic model for the propagation of the flow along the main river system. For reasons of computation time, merely time intervals of about one month around the downstream discharge peaks (at Lobith or Borgharen) according to HBV are simulated. SOBEK is thus used to improve the HBV-estimates of discharge peaks and in this way obtain more accurate discharge frequency curves.

In calibration uncertain parameters were varied until model predictions agree as good as possible with measured water levels and/or discharges. The calibration of the SOBEK-models was not combined with a GLUE procedure (as done for the hydrological HBV-models for the sub-basins) or any other form of uncertainty analysis. As a result a quantitative representation of the uncertainty in the parameters and/or the uncertainty in model predictions is not available. This is the main reason that in the present approach uncertainties in the hydrodynamic models have not been taken into account. As long as effects of flooding or dike breaks are absent or relatively small this is expected not to be a serious omission. The reason is that the total uncertainty in the predictions of the hydrodynamic models is in excess due to uncertainties in the model's input in the form of the lateral inflows produced by the hydrological models of the contributing sub-basins. As a matter of the sound physical/conceptual basis of the model the 'intrinsic' uncertainty in the models will be much smaller, and in the end (after combination of all uncertainty sources) hardly contribute to the total uncertainty.

In the hydraulic modelling of flows in the main river system SOBEK models are used in twofold. First a SOBEK version is used where (effects of) flooding, overflows, inundation, and or dike breaks are not included. This is not a serious "omission" for the Rhine and Meuse as long as flow conditions are simulated with return periods less than (approximately) 50 year (see Figure 4.4.1). However, for more extreme flow conditions overflow will take place and in particular in the German part of the Rhine relatively large effects on peak discharges are expected (Lammersen, 2004; IKSR, 2012).

To deal with this a second SOBEK model is applied as well, which takes into account the effects of flooding. Through comparison of the results of both SOBEK models the effect of flooding can be quantified.

Despite a sound physical basis of the hydrodynamic SOBEK models, several uncertainties remain. A relevant source of uncertainty is the model's schematisation (i.e. representation of the model's topography such as the river bed and flood plains). Examples of other identified uncertainties are roughness of the river bed and/or its floodplains (represented by friction coefficients) and uncertainties in the formulation of the effects of hydraulic structures.

In case also flooding is included in the modelling, other uncertainties become relevant. These refer to model parameters such as thresholds or dike heights at which flooding will occur, parameters determining when and where dikes may break, breach lengths, overflow/outflow velocities, area and/or volumes of storage areas, etc. In preceding studies the SOBEK models for the Rhine and the Meuse have been extensively calibrated (see e.g. Meijer, 2009).

The modelling of flooding involves additional parameters which are also uncertain. For the Rhine systematic variations of a set of such 'flooding parameters' have been made. Through GRADE frequency curves, the sensitivity of extreme Rhine discharges for the flooding mechanisms is established. This should be regarded as a sensitivity analysis to demonstrate the sensitivity to variations in the flooding parameters rather than a quantitative uncertainty analysis.

For the Meuse little is known about flooding and no model that includes flooding is (yet) available. Therefore neither an uncertainty nor a sensitivity analysis was carried out.

3 Method of the GRADE uncertainty analysis

In Chapter 2 the representation of the uncertainties in the main GRADE components has been outlined. In this chapter it is described how the uncertainties within the components are combined to obtain the 'total' uncertainty of the GRADE simulations of some 'target' variable. Here the focus is on extreme discharges associated to given return periods, or more generally a frequency-discharge curve which relates (extreme) discharges to corresponding return periods.

The main steps in the GRADE uncertainty analysis are listed below. In Appendix A these steps are described in much more detail together with the algorithms and mathematical formulas that are used to obtain the uncertainty estimates.

For the Rhine, the results of this uncertainty analysis will be presented in threefold: for the discharges at Lobith computed with the hydrological HBV model, secondly for the corresponding discharges based on the SOBEK model without flooding (via regression) and, thirdly, for the SOBEK model with flooding (also via regression).

A similar approach is followed for the Meuse, but now the uncertainty analysis is 'merely' presented in twofold since for the Meuse flooding is presently not taken into account.

3.1 The uncertainty matrix

As outlined in Chapter 2 the uncertainty in the climate is represented by a set of (11 or 24) different Weather Generator (WG) simulations and the uncertainty in the hydrological modeling by the set of five different HBV parameter combinations. Both sets represent the empirical probability distributions. The 'overall' uncertainty in the GRADE simulations is then governed by the set of mutual combinations of the elements of both sets. These combinations form an Uncertainty Matrix, which is illustrated in Table 3.1. The entries of the matrix represent a 'target' variable $Q(i,j)$. The target is computed with GRADE and represents the discharge that corresponds to a given return period. The entry $Q(i,j)$ is then the value of Q obtained when GRADE is run for the i -th weather generator member, and the j -th member of the HBV-parameter combinations.

Table 3.1 Illustration of the GRADE uncertainty matrix

HBV ► WG ▼	Par. Comb 5%	Par. Comb 25%	Par. Comb 50%	Par. Comb 75%	Par. Comb 95%
WG 1	Q(1,1)	Q(1,2)	Q(1,3)	Q(1,4)	Q(1,5)
WG 2	Q(2,1)	Q(2,2)	Q(2,3)	Q(2,4)	Q(2,5)
WG 3	Q(3,1)	Q(3,2)	Q(3,3)	Q(3,4)	Q(3,5)
WG 4	Q(4,1)	Q(4,2)	Q(4,3)	Q(4,4)	Q(4,5)
WG 5	Q(5,1)	Q(5,2)	Q(5,3)	Q(5,4)	Q(5,5)
WG 6	Q(6,1)	Q(6,2)	Q(6,3)	Q(6,4)	Q(6,5)
WG 7	Q(7,1)	Q(7,2)	Q(7,3)	Q(7,4)	Q(7,5)
WG 8	Q(8,1)	Q(8,2)	Q(8,3)	Q(8,4)	Q(8,5)
WG 9	Q(9,1)	Q(9,2)	Q(9,3)	Q(9,4)	Q(9,5)
WG 10	Q(10,1)	Q(10,2)	Q(10,3)	Q(10,4)	Q(10,5)
WG 11	Q(11,1)	Q(11,2)	Q(11,3)	Q(11,4)	Q(11,5)

3.2 Computation of the uncertainty matrix

Every entry $Q(i,j)$ in the uncertainty matrix involves a 20,000 year GRADE simulation. The $Q(i,j)$ typically represents the maximum discharge of the Rhine at Lobith (or at Borgharen for the Meuse) that corresponds to a given return period.

3.3 Variance reduction using Weissman’s method

In addition, Weissman’s procedure (Weissman, 1978) is applied to improve the estimates of discharges corresponding to return periods larger than 250 year (see Appendix A, Section A.3 for details).

3.4 Quantifying the uncertainties in the climate

For each HBV-parameter combination the corresponding column in the Uncertainty Matrix represents the uncertainty in the target variable Q due to the uncertainty in the climate represented by the set of Weather Generator simulations (See Table 3.2). From the $Q(i,j)$ -entries in each column a (marginal or conditional) estimate of the Q and its uncertainty can be derived. This provides a quantitative measure for solely the weather generator (i.e. climate) uncertainty. Comparing the results column wise (i.e. for each HBV parameter combination) gives an impression of the sensitivity for the parameter setting in the hydrological models.

Table 3.2 Column (marked in red) in the Uncertainty Matrix for computation of a marginal, climate induced, estimate and uncertainty of the target variable Q

HBV ► WG ▼	Par. Comb 5%	Par. Comb 25%	Par. Comb 50%	Par. Comb 75%	Par. Comb 95%
WG 1	Q(1,1)	Q(1,2)	Q(1,3)	Q(1,4)	Q(1,5)
WG 2	Q(2,1)	Q(2,2)	Q(2,3)	Q(2,4)	Q(2,5)
WG 3	Q(3,1)	Q(3,2)	Q(3,3)	Q(3,4)	Q(3,5)
WG 4	Q(4,1)	Q(4,2)	Q(4,3)	Q(4,4)	Q(4,5)
WG 5	Q(5,1)	Q(5,2)	Q(5,3)	Q(5,4)	Q(5,5)
WG 6	Q(6,1)	Q(6,2)	Q(6,3)	Q(6,4)	Q(6,5)
WG 7	Q(7,1)	Q(7,2)	Q(7,3)	Q(7,4)	Q(7,5)
WG 8	Q(8,1)	Q(8,2)	Q(8,3)	Q(8,4)	Q(8,5)
WG 9	Q(9,1)	Q(9,2)	Q(9,3)	Q(9,4)	Q(9,5)
WG 10	Q(10,1)	Q(10,2)	Q(10,3)	Q(10,4)	Q(10,5)
WG 11	Q(11,1)	Q(11,2)	Q(11,3)	Q(11,4)	Q(11,5)

3.5 Quantifying the uncertainties in the hydrological models

Similar to the description in Section 3.4 the Uncertainty Matrix can be evaluated along the rows. In this case, the estimate and uncertainty of the target variable Q are derived for a given state of the climate (represented by a WG member), see Table 3.3. These marginal estimates (separately computed for each WG-row) quantify the uncertainty in Q due to (the uncertainties in) the hydrological models. Here the dependency or sensitivity for the various WG-members can be evaluated by comparing the different rows. In summary, from the row wise and column wise (as described in Section 3.4) evaluations, the contributions to the uncertainties in Q , from the climate on one hand, and the hydrological modeling on the other, can be compared and ranked.

Table 3.3 Row (marked in red) in the Uncertainty Matrix for computation of a marginal, hydrological model induced, estimate and uncertainty of the target variable Q

HBV ► WG ▼	Par. Comb 5%	Par. Comb 25%	Par. Comb 50%	Par. Comb 75%	Par. Comb 95%
WG 1	Q(1,1)	Q(1,2)	Q(1,3)	Q(1,4)	Q(1,5)
WG 2	Q(2,1)	Q(2,2)	Q(2,3)	Q(2,4)	Q(2,5)
WG 3	Q(3,1)	Q(3,2)	Q(3,3)	Q(3,4)	Q(3,5)
WG 4	Q(4,1)	Q(4,2)	Q(4,3)	Q(4,4)	Q(4,5)
WG 5	Q(5,1)	Q(5,2)	Q(5,3)	Q(5,4)	Q(5,5)
WG 6	Q(6,1)	Q(6,2)	Q(6,3)	Q(6,4)	Q(6,5)
WG 7	Q(7,1)	Q(7,2)	Q(7,3)	Q(7,4)	Q(7,5)
WG 8	Q(8,1)	Q(8,2)	Q(8,3)	Q(8,4)	Q(8,5)
WG 9	Q(9,1)	Q(9,2)	Q(9,3)	Q(9,4)	Q(9,5)
WG 10	Q(10,1)	Q(10,2)	Q(10,3)	Q(10,4)	Q(10,5)
WG 11	Q(11,1)	Q(11,2)	Q(11,3)	Q(11,4)	Q(11,5)

3.6 Combination of the uncertainties in the climate and the hydrological models

The differences in Q along the columns and rows of the Uncertainty Matrix as described above in Sections 3.4 and 3.5 are combined to obtain an overall uncertainty estimate for the target variable Q.

4 GRADE uncertainty analysis for discharge extremes for the Rhine at Lobith

The uncertainty analysis described in Chapter 3 has been applied to the GRADE system developed for the Rhine and the results are presented in this chapter. This uncertainty analysis fully concentrates on the extreme discharges at Lobith, at the downstream boundary of the GRADE model for the Rhine. From the GRADE simulations annual maximum values of the Lobith discharges were selected. These were then used in an analysis to construct the Lobith discharge frequency curves. In these curves annual maximum values are plotted versus the associated return period. Of major importance is the uncertainty in the GRADE discharge estimates at Lobith for return periods up to 10,000 years or longer

As mentioned in the previous chapter, the uncertainty analysis for discharge frequency curves at Lobith is carried out in threefold. In Section 4.1 the results are presented for the case that no hydrodynamic SOBEK modeling is used (i.e. the discharges according to the HBV hydrological model). In Section 4.2 the uncertainties in, these discharge frequency curves are again presented but now with SOBEK as the hydrodynamic model for an improved simulation of the flood propagation along the main river. With this SOBEK model possible effects of overflows are not yet taken into account, however. In Section 4.3 the results of the uncertainty analysis are presented for the SOBEK version where the effects of flooding are also modeled.

In these uncertainty analyses no uncertainties in the SOBEK models have been taken into account. Some effects of variations of uncertain parameters in the modeling of flooding have been established by Udo and Termes (2013). The results of their sensitivity analysis (rather than uncertainty analysis) are summarized in Section 4.4 and provide important evidence for the significance of flooding induced effects on the Lobith discharge frequency curve.

4.1 HBV estimates and uncertainties of extreme discharges at Lobith

In this section the results are presented of the GRADE uncertainty analysis for extreme discharges at Lobith as computed with the hydrological HBV-models in the GRADE system for the Rhine. The GRADE simulations covered a time period of 20,000 years. From the generated/simulated time series the annual maxima at Lobith were selected, and from this selection the annual extreme $Q(RP)$ associated to various return periods RP was determined empirically for return periods less or equal to 250 year, and with Weissman's procedure for longer return periods.

Below, the results of the uncertainty analysis are displayed by means of the following tables and figures:

- Table 4.1.1 presents the Uncertainty Matrix (UM) for the annual maximum discharges at Lobith with return period (*RP*) of 1250 years. These are thus the GRADE results for every combination of the climate and a HBV-parameter set.
- Similarly Table 4.1.2 shows this Uncertainty Matrix for *RP* = 4000 years.
- In Table 4.1.3 estimates of the annual maximum discharge at Lobith are listed for a set of representative *RPs* in the range of 5 to 10.000 years. The uncertainty in these estimates is presented as a spread (i.e. the standard deviation) and as a 95% confidence interval.
- In graphical form the dependency of $Q(RP)$ on the return period is shown in Figure 4.1.1. In this probability plot (or frequency curve) the bounds of the 95% confidence interval for the $Q(RP)$ are also plotted. Two confidence intervals are: (i) for the overall uncertainty in the $Q(RP)$, i.e. the combined uncertainties of both Weather Generator (i.e. climate) and the hydrological HBV-models, and (ii) for the uncertainty due to 'solely' the uncertainty in the hydrological models.

Table 4.1.1 GRADE (without SOBEK) Uncertainty Matrix for the yearly maximum discharge at Lobith (Rhine) for return period $RP=1250$ years, according to the Weather Generator plus the HBV models.

HBV ► WG ▼	5% Par. Comb.	25% Par. Comb.	50% Par. Comb.	75% Par. Comb.	95% Par. Comb.	Mean HBV (m_{HBV})	Spread HBV (s_{HBV})
WG Ref.	16673	16218	16702	16999	16354	16629	295
WG 1	16789	16278	16886	17119	16402	16745	330
WG 2	17033	16612	17122	17342	16707	17009	286
WG 3	17363	16808	17359	17639	16949	17260	318
WG 4	16898	16348	16956	17127	16462	16799	313
WG 5	17076	16602	17131	17396	16721	17028	306
WG 6	16648	16177	16685	16905	16272	16576	285
WG 7	16954	16433	17002	17213	16551	16871	307
WG 8	16151	15709	16207	16467	15850	16117	288
WG 9	16148	15780	16210	16517	15887	16153	279
WG 10	16873	16418	17006	17215	16530	16861	315
WG 11	16885	16388	16965	17179	16503	16829	311
Mean WG (m_{WG})	16802	16323	16866	17102	16440		
Spread WG (s_{WG})	1113	1008	1100	1065	1008		
Overall Mean (m): 16750 [m^3/s] Overall Standard Deviation (s): 1102 [m^3/s]							
95% symmetric confidence interval Q_{Lobith}^{Max} for return period 1250 years: (14590, 18910) [m^3/s]							

Table 4.1.2 GRADE (without SOBEK) Uncertainty Matrix for the yearly maximum discharge at Lobith (Rhine) for return period RP=4000 years, according to the Weather Generator plus the HBV models.

HBV ► WG ▼	5% Par. Comb	25% Par. Comb	50% Par. Comb	75% Par. Comb	95% Par. Comb.	Mean HBV (m_{HBV})	Spread HBV (s_{HBV})
WG Ref.	18033	17473	18089	18382	17676	17975	343
WG 1	18262	17689	18481	18644	17860	18253	386
WG 2	18371	17962	18522	18697	18030	18370	298
WG 3	18935	18223	18837	19133	18409	18732	349
WG 4	18412	17694	18476	18515	17801	18219	362
WG 5	18630	18062	18635	18955	18166	18534	347
WG 6	17947	17445	17970	18154	17507	17841	287
WG 7	18498	17832	18631	18703	17971	18377	371
WG 8	17352	16834	17409	17657	17044	17298	309
WG 9	17331	16924	17459	17762	17084	17366	316
WG 10	18222	17734	18506	18589	17813	18246	369
WG 11	18364	17780	18478	18627	17901	18279	346
Mean WG (m_{WG})	18211	17653	18309	18494	17780		
Spread WG (s_{WG})	1494	1310	1448	1384	1267		
Overall Mean (m): 18138 [m^3/s] Overall Standard deviation (s): 1421 [m^3/s]							
95% symmetric confidence interval Q_{Lobith}^{Max} for return period 4000 years: (15350, 20920) [m^3/s]							

Table 4.1.3 GRADE (without SOBEK) estimates for the discharge at Lobith (Rhine) and its uncertainty for return periods between 5 and 10,000 years. The listed discharges and uncertainty measures have been rounded off to the nearest multiple of 10.

Return Period [years]	Estimate of $Q_{Lobith}^{Max}(RP)$ [m^3/s]	Spread in $Q_{Lobith}^{Max}(RP)$ [m^3/s]	Symmetric 95% confidence interval for $Q_{Lobith}^{Max}(RP)$ [m^3/s]	
			Lower Bound	Upper Bound
5	8430	480	7490	9370
10	9800	550	8730	10880
20	11020	630	9790	12260
50	12480	760	10990	13870
100	13510	830	11890	13510
250	14830	760	13340	16310
500	15660	880	13920	17390
1250	16750	1100	14590	18910
4000	18140	1420	15350	20920
10000	19230	1690	15920	22540

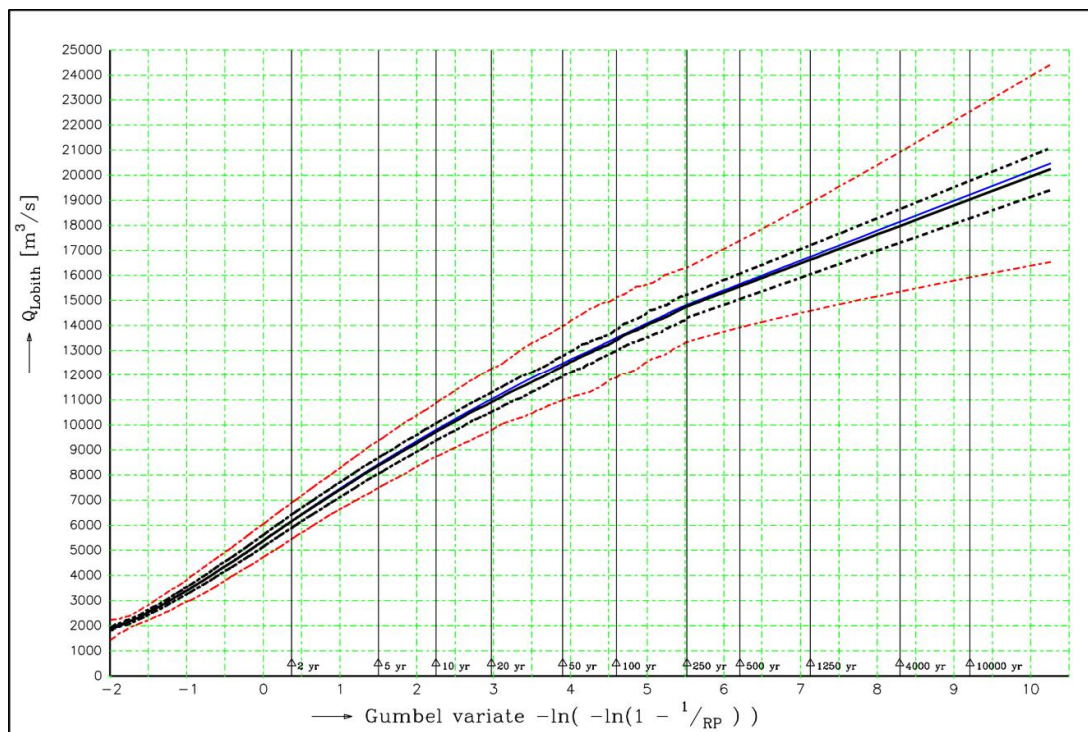


Figure 4.1.1 Frequency curves for extreme discharges of the Rhine at Lobith, according to GRADE (without SOBEK). The solid curve in blue represents the estimate of $Q(RP)$ for the various return periods RP . The lower and upper bounds of the 95% confidence interval are denoted by the red coloured dashed curves. In the computation of these curves the uncertainty in both the climate and in the HBV-models are taken into account. The curves in black give the $Q(RP)$ and the confidence intervals for “merely” the uncertainty in the HBV-models.

Main conclusions from the tables and figures:

For every return period the total uncertainty in the corresponding GRADE estimate of the extreme discharge $Q(RP)$ of the Rhine at Lobith is dominated by the climate uncertainty, i.e. the uncertainty in the rainfall and temperature. Moreover, the larger the RP the larger the relative contribution of the uncertainty in the climate to the total uncertainty in $Q(RP)$. As a result the uncertainty in $Q(RP)$ is for high return periods also hardly sensitive for weights assigned to the five HBV-model parameter combinations.

Below, a more detailed analysis and discussion of the tables, figures and methods used is given.

As described in Section 3.3 a Weissman ‘smoothing’ was applied as variance reduction technique for improving the estimates of (the mean and spread of) discharges for long return periods. The Weissman recipe was applied to the subset of extremes with $RP > 250$ years. In this way the values for $RP > 250$ in the tables are Weissman estimates rather than ‘empirical’ values derived directly from the GRADE simulations.

In the last two columns of the UM the results of the evaluation of the uncertainty in the HBV models (i.e. evaluated over the rows of the UM) can be found in the form of a mean (m_{HBV}) and a spread (s_{HBV}). These are computed according to:

$$m_{HBV}(i) = \sum_{j=1}^5 w_j \cdot Q(i, j) \quad (4.1.1a)$$

$$s_{HBV}(i) = \sqrt{\sum_{j=1}^5 w_j \cdot (Q(i, j) - m_{HBV}(i))^2} \quad (4.1.1b)$$

The w_j in these equations is the weight assigned to the j -th HBV parameter set.

Similarly, the mean (m_{WG}) and spread (s_{WG}) that are obtained from the uncertainty in the climate (i.e. evaluated over the columns) are listed in the second and third last rows of the tables respectively. These are computed according to the formulas:

$$m_{WG}(j) = \frac{1}{N} \sum_{i=1}^N Q(i, j) \quad (4.1.2a)$$

$$s_{WG}(j) = \sqrt{\frac{N-1}{N} \cdot \sum_{i=1}^N (Q(i, j) - m_{WG}(j))^2} \quad (4.1.2b)$$

N is the number of synthetically generated weather series using a Jackknife resampling procedure. In the present case $N=11$. For the theoretical background of these equations one is referred to Appendix A.

In the last row but one of the tables the mean (m) and spread (s) after the combination of the uncertainties in the climate and in the hydrological modelling are presented (in bold). This overall mean and standard deviation are calculated from the mean and standard deviation for each HBV parameter set, taking into account the weights w_j (see Appendix A):

$$m = \sum_{j=1}^5 w_j \cdot m_{WG}(j) \quad (4.1.3a)$$

$$s = \sqrt{\sum_{j=1}^5 w_j \cdot [m_{WG}(j) - m]^2 + \sum_{j=1}^5 w_j \cdot s_{WG}^2(j)} \quad (4.1.3b)$$

The spread of Equation 4.1.3b gives the overall uncertainty estimate for a specific $Q(RP)$. The symmetric 95% confidence interval that can be derived for $Q(RP)$ from the mean and spread (assuming a normal distribution) is listed in the last row of the tables.

Table 4.1.1, shows that the contribution of the uncertainty in the climate to the spread in $Q(1250)$ is considerably larger than the contribution of the uncertainty in the hydrological models. In fact, the weighted average of the spreads listed in the last row (representing the average climate induced uncertainty) is $1059 \text{ m}^3/\text{s}$ and is almost 3.5 times as large as the weighted average of $303 \text{ m}^3/\text{s}$ of the spreads $s_{HBV}(i)$ listed in the last columns (representing the averaged HBV-parameter induced uncertainty). The spread in the overall estimate of $Q(RP)$ amounts $1102 \text{ m}^3/\text{s}$ and is thus only slightly larger than the average of the climate induced spreads.

The overall spread of $1102 \text{ m}^3/\text{s}$ in $Q(1250)$ of $16,750 \text{ m}^3/\text{s}$ corresponds to a relative spread of 6.6%.

The dominance of the uncertainty in the climate has also the consequence that the overall estimate for $Q(RP)$ and its spread is not very sensitive for the weights assigned to the five HBV parameter combinations. For example (and again for $RP=1250$ years), if uniform weights would have been used a value of $16,707 \text{ m}^3/\text{s}$ would be found for $Q(RP)$ (instead of $16,750 \text{ m}^3/\text{s}$) and $1098 \text{ m}^3/\text{s}$ for the overall spread in this estimate.

The Uncertainty Matrix (UM) shows that $Q(RP)$ does not monotonically increase along the rows of the UM. Such a monotonic increase would, however, be expected from the selection criterion used in the GLUE analysis to select the present five representatives out of all behavioural HBV-parameter combinations. In this criterion the representatives were associated to quantiles in a set of extreme discharges, corresponding to a 10 year return period, and computed with observed weather data as input for each of the major sub-basins of the Rhine. For the return period of 1250 years, and synthetic rather than observed weather data, the monotonic dependency of the HBV-parameter sets and the extreme discharge does not persist. One reason may be that in the selection procedure extremes of a much longer return period should have been adopted. Further, the selection of the representatives was done for each major sub-basin of the Rhine separately. In second instance “quantile wise” combinations were made to reduce the number of parameter sets to five for the whole river basin as well (see Section 2.2). It may be possible that for individual sub-basins the ordering is preserved for higher return periods, but is lost in the quantile-wise combination.

This remains a hypothesis since no Uncertainty Matrices were made (neither for $RP=1250$ years nor for other return periods significantly higher than 10 years) for extreme discharges in the separate major sub-basins of the Rhine to verify when and where monotony is lost.

The aforementioned findings also tend to hold for the Uncertainty Matrix for $RP=4000$ years that is listed in Table 4.1.2. $Q(4000)$ is estimated as $18,138 \text{ m}^3/\text{s}$. The spread in this estimate amounts $1421 \text{ m}^3/\text{s}$. The relative spread of 7.8% is somewhat larger than the one for $RP=1250$ years (6.6%). The total uncertainty in $Q(RP)$ is again dominated by the uncertainty in the Weather Generator (i.e. climate). The contributions from HBV and the Weather Generator are respectively 337 and $1380 \text{ m}^3/\text{s}$. The uncertainty induced by the climate is then 4 times as large as the uncertainty arising from the hydrological models.

The increase of the relative uncertainty with increasing RP can also be recognised from the spreads and confidence intervals for other return periods in Table 4.1.3. For a return period of 10,000 years the relative spread increases to 8.8%.

In graphical form the dependency of $Q(RP)$ on RP is shown in Figure 4.1.1 through a return period plot. This plot highly confirms the findings so far extracted from the tables.

The blue solid curve in this figure shows the estimate of $Q(RP)$ after combining results for the climate and the HBV-parameter combinations within the UM. The overall 95% (symmetric) confidence band is marked by the two dashed red curves.

In the same way the black curves in Figure 4.1.1 represent $Q(RP)$ and its 95% confidence band when only the uncertainty in the HBV-models is taken into account. In this case the 20,000-year reference Weather Generator (WG) data was used in combination with the five HBV-variations. The results of the uncertainty analysis are then as listed in the upper row in the UM (marked in green in the UM of the Table 4.1.1 and Table 4.1.2). The frequency curve derived from the reference WG data (black solid curve in Figure 4.1.1) hardly deviates from the one averaged over the various WG-variations (blue solid curve).

The width of the confidence band marked by the two black dashed lines is substantially smaller than the overall confidence band. At the same time Figure 4.1.1 also clearly indicates that for increasing *RP* the width of the overall confidence band grows more than the width of the confidence band representing the uncertainty in the HBV models. This means that the larger the *RP* the larger the relative contribution of the uncertainty in the climate to the total uncertainty.

4.2 SOBEK estimates and uncertainties of extreme Lobith discharges (without flooding)

The uncertainty analysis described in Section 4.1 was repeated but now using the Lobith peak discharges according to SOBEK. In this case a SOBEK-version is used in which effects of flooding in the German part of the river are not included.

The starting point of the analysis is again the Uncertainty Matrix with in the entries the SOBEK computed annual discharge extremes for some return period of interest. Note that because of the large computation time of SOBEK these SOBEK extremes have not been generated by re-computing all discharge events that correspond with the annual maxima computed by HBV. In fact, SOBEK discharge extremes were only generated for the 50,000-year reference GRADE simulation (i.e. the reference WG simulation combined with the reference (i.e. 50%)HBV parameter set). This provided 50,000 (HBV, SOBEK)-pairs of annual extremes.

A regression was applied to obtain an analytical formula that, for a given HBV discharge extreme, provides an estimate for the corresponding value that would be computed with SOBEK. This regression is described and illustrated in Appendix B.

The regression relation is thus derived from the 50,000-year reference GRADE simulation (which provides both the HBV and SOBEK annual maxima). It is assumed, however, that this regression also provides an accurate description for the relation of the HBV and SOBEK discharges for all other combinations of the Weather Generator and HBV-parameters. The regression is thus applied to every entry in the HBV uncertainty matrix (as listed in Section 4.1) to obtain the SOBEK uncertainty matrix (presented in Table 4.4).

The results are presented in the Tables 4.4 to 4.6 and Figure 4.2 in a similar way as in the preceding section. The same conclusions can be derived as in the previous section because of the almost linear relationship between the HBV and corresponding SOBEK discharges. This can be observed from the (red) regression curve shown in Figure B.1.1 in Appendix B.

Table 4.2.1 Uncertainty Matrix for the discharge of the Rhine at Lobith for return period RP=1250 years, according to GRADE (SOBEK without flooding)

HBV ► WG ▼	5% Par. Comb	25% Par. Comb	50% Par. Comb	75% Par. Comb	95% Par. Comb.	Mean HBV (m_{HBV})	Spread HBV (s_{HBV})
WG Ref.	16085	15612	16115	16426	15752	16039	308
WG 1	16205	15673	16304	16551	15800	16158	344
WG 2	16460	16018	16554	16787	16118	16435	301
WG 3	16813	16231	16811	17107	16378	16707	336
WG 4	16323	15752	16384	16566	15870	16222	326
WG 5	16510	16012	16568	16847	16137	16460	322
WG 6	16059	15568	16098	16327	15666	15984	298
WG 7	16376	15833	16425	16649	15956	16290	320
WG 8	15538	15082	15595	15866	15226	15503	298
WG 9	15536	15157	15602	15920	15267	15542	289
WG 10	16299	15821	16436	16657	15939	16285	330
WG 11	16306	15787	16390	16615	15907	16248	326
Mean WG (m_{WG})	16220	15721	16288	16536	15842		
Spread WG (s_{WG})	1168	1050	1156	1125	1054		
Overall Mean (m): 16167 [m^3/s] Overall Standard Deviation (s): 1156 [m^3/s]							
95% symmetric confidence interval Q_{Lobith}^{Max} for return period 1250 years: (13900, 18430) [m^3/s]							

Table 4.2.2 Uncertainty Matrix for the discharge of the Rhine at Lobith for return period RP=4000 years, according to GRADE (SOBEK without flooding)

HBV ► WG ▼	5% Par. Comb	25% Par. Comb	50% Par. Comb	75% Par. Comb	95% Par. Comb.	Mean HBV (m_{HBV})	Spread HBV (s_{HBV})
WG Ref.	17485	16895	17542	17858	17106	17424	364
WG 1	17721	17112	17945	18129	17288	17708	410
WG 2	17847	17404	18006	18199	17480	17845	322
WG 3	18450	17693	18353	18674	17889	18240	376
WG 4	17886	17133	17955	18010	17247	17689	383
WG 5	18120	17511	18130	18472	17626	18019	372
WG 6	17397	16862	17422	17622	16930	17286	307
WG 7	17968	17264	18103	18195	17412	17841	393
WG 8	16762	16219	16821	17087	16433	16706	326
WG 9	16743	16317	16876	17198	16480	16779	333
WG 10	17697	17171	17988	18090	17260	17718	393
WG 11	17831	17209	17952	18118	17340	17743	371
WG Mean	17675	17081	17777	17981	17217		
WG Spread	1586	1382	1538	1480	1345		
Overall Mean: 17598 [m^3/s] Overall Standard deviation: 1510 [m^3/s]							
95% symmetric confidence interval Q_{Lobith}^{Max} for return period 4000 years: (14640, 20560) [m^3/s]							

Table 4.2.3 GRADE (SOBEK without flooding) estimates for the discharge at Lobith (Rhine) and its uncertainty for return periods between 5 and 10,000 years. The listed discharges and uncertainty measures have been rounded off to the nearest multiple of 10

Return Period [years]	Estimate of $Q_{Lobith}^{Max}(RP)$ [m^3/s]	Spread in $Q_{Lobith}^{Max}(RP)$ [m^3/s]	Symmetric 95% confidence interval for $Q_{Lobith}^{Max}(RP)$ [m^3/s]	
			Lower Bound	Upper Bound
5	8080	440	7210	8950
10	9350	510	8350	10350
20	10490	590	9330	11660
50	11880	730	10450	13310
100	12880	810	11290	14460
250	14180	760	12690	15680
500	15040	910	12250	16820
1250	16170	1160	13900	18430
4000	17600	1510	14640	20560
10000	18720	1810	15190	22260

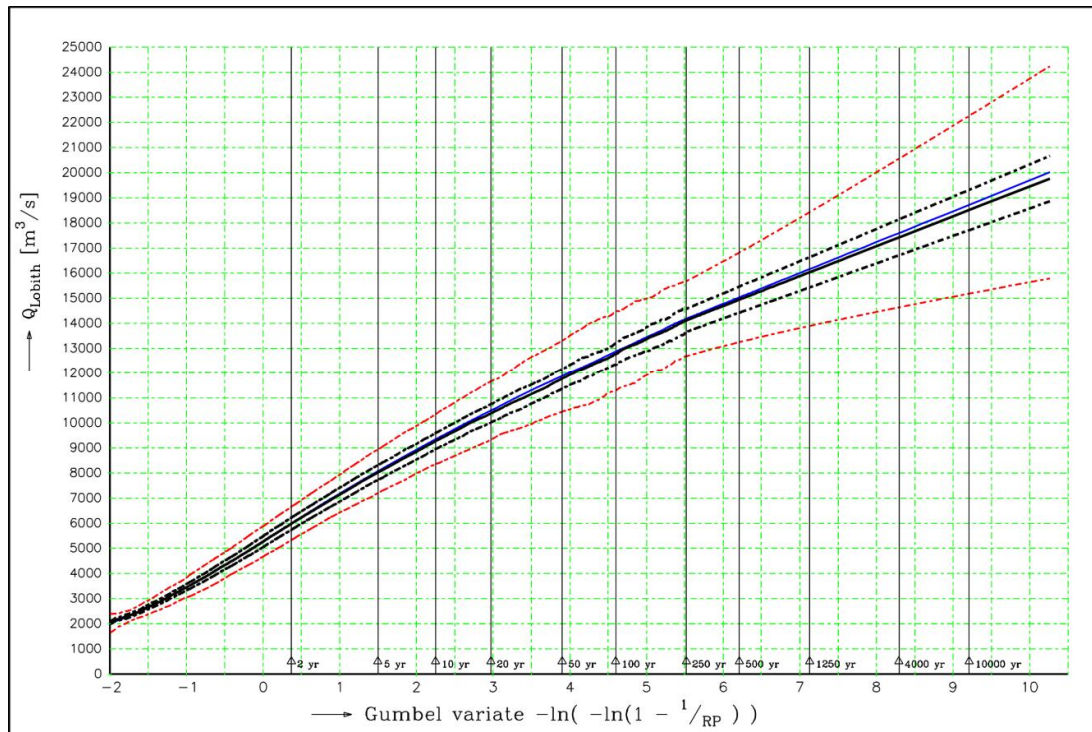


Figure 4.2.1 Frequency curve for extreme discharges of the Rhine at Lobith, according to GRADE (SOBEK without flooding). The solid curve in blue represents the estimate of $Q(RP)$ for the various return periods RP . The lower and upper bounds of the 95% confidence interval are denoted by the red coloured dashed curves. In the computation of these curves the uncertainty in both the climate and in the HBV-models are taken into account. The curves in black give the $Q(RP)$ and the confidence intervals for “merely” the uncertainty in the HBV-models

4.3 SOBEK estimates and uncertainties of extreme Lobith discharges (with flooding)

In this section the results of the GRADE uncertainty analysis are presented for the case that the Lobith peak discharges are again computed with SOBEK but now with the version in which effects of flooding are also taken into account.

Just as in Section 4.2, a regression formula was applied to convert the HBV computed values of the Lobith discharge extremes to a corresponding SOBEK(+flooding) value. This regression is described and illustrated in Appendix B, see Figure B.2.1. This figure shows that effects of flooding become notable for discharges greater than about 12,000 m^3/s . According to GRADE/SOBEK this corresponds to a return period of about 50 year.

The results of the subsequent uncertainty analysis can be found below, and are summarised by means of similar tables and figures as were presented in the preceding sections. From these results similar conclusions can be derived:

For discharges less than (about) 12,000 m^3/s (and correspondingly return periods less than about 50 year) the present extreme Lobith discharges will virtually be the same as those for the SOBEK model without flooding (and as presented in Section 4.2). For long(er) return periods the estimates of the $Q(RP)$ are now substantially smaller, however. At the same time the uncertainties in these estimates are less as well.

From a “mathematical” viewpoint the reason of this reduction can be explained from the relation between the SOBEK with and without flooding computed discharges. This relation is highly linear as can be seen from Figure B.3.2 in Appendix B. The slope of the curve is less than one which explains the smaller $Q(RP)$ that are now found. This slope also determines the ratio of the uncertainties in these estimates, and for this reason also a much smaller spread and width of the confidence intervals are now found.

From a physical viewpoint it can be argued that the reduction of $Q(RP)$ and its uncertainty will be present as soon as a certain discharge threshold for flooding is exceeded. The volume available for storage of the flooded water will be that large that it highly limits the variability of the discharge and the maxima occurring at Lobith. At the same time flooded volumes that reflow into the river will have effects at the Lobith discharge only long after the time epoch of the maxima.

Table 4.3.1 Uncertainty Matrix for the discharge of the Rhine at Lobith for return period $RP=1250$ years, according to GRADE (SOBEK with flooding)

HBV ► WG▼	5% Par. Comb.	25% Par. Comb.	50% Par. Comb.	75% Par. Comb.	95% Par. Comb.	Mean HBV (m_{HBV})	Spread HBV (s_{HBV})
WG Ref.	14196	14022	14209	14309	14080	14177	108
WG 1	14237	14049	14282	14350	14102	14222	119
WG 2	14316	14178	14347	14413	14208	14307	93
WG 3	14420	14227	14409	14498	14280	14377	103
WG 4	14273	14056	14290	14338	14101	14225	116
WG 5	14322	14158	14336	14426	14196	14302	103
WG 6	14181	14006	14193	14268	14041	14151	103
WG 7	14303	14110	14327	14383	14154	14269	110
WG 8	14004	13820	14028	14124	13890	13989	115
WG 9	14003	13845	14025	14142	13898	13999	112
WG 10	14243	14088	14303	14363	14126	14245	111
WG 11	14269	14094	14297	14365	14134	14247	107
Mean WG (m_{WG})	14234	14057	14258	14334	14103		
Spread WG (s_{WG})	389	384	379	345	365		
Overall Mean (m): 14212 [m^3/s] Overall Standard deviation (s): 385 [m^3/s]							
95% symmetric confidence interval Q_{Lobith}^{Max} for return period 1250 years: (13460, 14970) [m^3/s]							

Table 4.3.2 Uncertainty Matrix for the discharge of the Rhine at Lobith for return period $RP=4000$ years, according to GRADE (SOBEK with flooding)

HBV ► WG▼	5% Par. Comb.	25% Par. Comb.	50% Par. Comb.	75% Par. Comb.	95% Par. Comb.	Mean HBV (m_{HBV})	Spread HBV (s_{HBV})
WG Ref.	14788	14621	14814	14868	14701	14769	94
WG 1	14875	14737	14983	14967	14802	14892	102
WG 2	14845	14777	14898	14912	14774	14855	61
WG 3	15022	14818	14958	15024	14878	14939	79
WG 4	14915	14676	14926	14873	14701	14825	106
WG 5	14952	14811	14928	15013	14817	14912	81
WG 6	14738	14620	14736	14764	14618	14702	63
WG 7	14962	14764	15032	14971	14802	14920	109
WG 8	14586	14425	14603	14653	14522	14566	85
WG 9	14575	14447	14625	14694	14521	14588	93
WG 10	14784	14684	14918	14879	14683	14815	102
WG 11	14895	14754	14931	14932	14775	14869	80
Mean WG (m_{WG})	14832	14683	14867	14880	14717		
Spread WG (s_{WG})	446	409	436	378	362		
Overall Mean (m): 14807 [m^3/s] Overall Standard Deviation (s): 414 [m^3/s]							
95% symmetric confidence interval Q_{Lobith}^{Max} for return period 4000 years: (14000, 15620) [m^3/s]							

Table 4.3.3 GRADE (SOBEK with flooding) estimates for the discharge at Lobith (Rhine) and its uncertainty for return periods between 5 and 10,000 years. The listed discharges and uncertainty measures have been rounded off to the nearest multiple of 10

Return Period [years]	Estimate of $Q_{Lobith}^{Max}(RP)$ [m^3/s]	Spread in $Q_{Lobith}^{Max}(RP)$ [m^3/s]	Symmetric 95% confidence interval for $Q_{Lobith}^{Max}(RP)$ [m^3/s]	
			Lower Bound	Upper Bound
5	8070	440	7210	8930
10	9320	500	8340	10300
20	10420	570	9310	11530
50	11700	640	10440	12960
100	12520	630	11290	13750
250	13390	420	12560	14210
500	13740	400	12970	14520
1250	14210	390	13460	14970
4000	14810	410	14000	15620
10000	15280	470	14360	16190

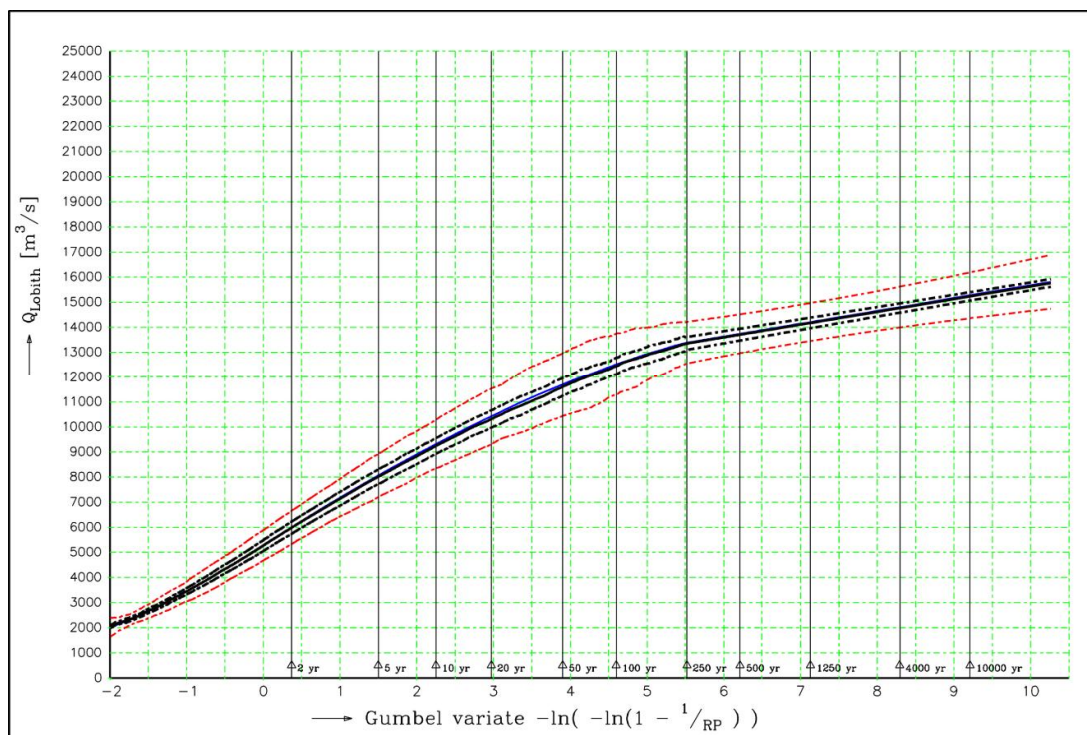


Figure 4.3.1 Frequency curve for extreme discharges of the Rhine at Lobith, according to GRADE (SOBEK with flooding). The solid curve in blue represents the estimate of $Q(RP)$ for the various return periods RP . The lower and upper bounds of the 95% confidence interval are denoted by the red coloured dashed curves. In the computation of these curves the uncertainty in both the climate and in the HBV-models are taken into account. The curves in black give the $Q(RP)$ and the confidence intervals for “merely” the uncertainty in the HBV-models

4.4 Sensitivity analysis of flooding parameters in the SOBEK model

Effects of flooding and/or overflows depend on several parameters as for example heights of thresholds or dikes, width of inflow apertures, storage capacity of inflow areas, bottom heights of the inflow areas, dike strength/break parameters, etc. For the modelling of these effects, as presently done within SOBEK, proper estimates for such flooding parameters can usually be obtained from bed elevation maps. Uncertainties may remain, however.

For the present SOBEK model for the Lower Rhine (with flooding included) a model calibration was carried out to further improve the ‘prior’ estimates for the flooding parameters. For extreme discharge conditions that lead to flooding no real measurements are available. Therefore water level and discharge predictions of a corresponding detailed 2D WAQUA model were used as ‘pseudo’ measurements in the calibration of the flooding parameters in the SOBEK model (Vieira da Silva et al., 2013). As a matter of its sound physical/conceptual basis, and high resolution in the 2D-spatial and temporal schematisation, the WAQUA model is expected to provide reasonably accurate predictions of flooding effects (at least for Andernach discharges up to 17.000 m^3/s).

For detailed description of the set up and results of the SOBEK model with flooding and overflows in the German part of the Rhine one is referred to Udo and Termes (2013).

The SOBEK-model with the in the past through a calibration derived estimates for the flooding parameters was used in the GRADE simulation described in the previous Section 4.3. Compared to the corresponding results obtained with a SOBEK model without flooding (Section 4.2) large effects were found in the estimates of extreme discharges at Lobith. Additionally to the tables and figures presented in Sections 4.2 and 4.3 this effect of taking flooding into account is in an alternative way depicted in Figure 4.4.1. This figure shows for Lobith the difference $\Delta Q_{Max}(RP)$ of extreme discharges as function of the return period RP .

This difference $\Delta Q_{Max}(RP)$ is defined by:

$$\Delta Q_{Max}(RP) := Q_{Max}(RP) \Big|_{SOBEK+Flooding} - Q_{Max}(RP) \Big|_{SOBEK-Flooding} .$$

In the remainder of this section the effect of variations in the various flooding parameters will be examined. In this variational analysis the setting of the flooding parameters as used in Section 4.3 is considered as reference. The effects of variations in this reference setting on the $Q_{Max}(RP)$ at Lobith are compared to the $Q_{Max}(RP)$ for the reference setting (in contrast to Figure 4.4.1 where the $Q_{Max}(RP)$ of the model with flooding was compared to the SOBEK model without flooding).

In this way the sensitivity of the Lobith extreme discharges to variations in the flooding parameters is established. This may give important insight into the extent that uncertainties in these parameters may contribute to (and/or increase) the total uncertainty in extreme Lobith discharges (i.e.: the relevance of taking uncertainties in flooding mechanisms into account).

For all uncertain flooding parameters a “physical realistic” range of potential variation around their reference value was determined. In the present sensitivity analysis, GRADE runs were only carried out for a minimum and a maximum variation of each parameter within this range. In the end this resulted in eight GRADE simulations (Rhine, SOBEK+Flooding) concerning the following four types of flooding parameters (Udo and Termes, 2013):

- 1 Heights of the dikes along the Oberrhein trajectory (from Maxau to Andernach) and Niederrhein (Andernach to Lobith).
The ('guard') heights were varied in twofold: first, an increase of these heights with +0.5 m, and secondly an 'increase' with -0.5 m. Note that such an increase or decrease with 0.5 m was applied uniformly, i.e. simultaneously to all river sections with potential flooding.
- 2 The width of inflow opening(s) in case of overflows of dikes.
These inflow openings were also varied in twofold and again in a uniform way. In one variation they were all increased with 25% (of the reference setting), and in the other 'increased' with -50%.
- 3 The available storage capacity in the form of the area covered by retention areas and/or flood areas behind dikes.
Also the storage capacity parameters were varied in twofold, and again in a uniform way: first an increase with 50% and secondly an 'increase' of -50%.
- 4 Bottom height of the retention areas and/or flood areas.
In a first variation all these bottom heights were increased with +1 m, and in a second variation 'increased' with -1 m.

No GRADE computations with joint variations of the various types of flooding parameters were carried out.

The effect of these eight variations of the flooding parameters on extreme Lobith discharges is graphically illustrated in Figure 4.4.1. The figure shows the increase or decrease $\Delta Q_{Max}(RP)$ relative to the $Q_{Max}(RP)$ that was found for the reference setting of the flooding parameters. In a formula this $\Delta Q_{Max}(RP)$ reads:

$$\Delta Q_{Max}(RP) := Q_{Max}(RP) \Big|_{SOBEK, FloodingVariation} - Q_{Max}(RP) \Big|_{SOBEK, FloodingReference}$$

From the **red** curves in Figure 4.4.1 it is readily recognised that within the presently adopted range of variations the largest effects are found for the guard heights of the dikes.

Also a high sensitivity is found for the storage capacity of the inflow areas (**blue** curves).

For the bottom height of the inflow areas (**green** curves) effects are also notable. When the bottom height is increased with +1 m a significant increase of the $Q_{Max}(RP)$ (compared to the reference setting) at Lobith is found for extremely high return periods only. Remarkably, an "increase" of the bottom height with -1 m yields about the same results as the increase with 1 m.

Effects of the inflow width variations (**black** curves) tend to be limited, particular when compared to the effects of the dike height and storage capacity variations.

It must be emphasized that so far no probabilities were assigned to the (variations in the) flooding parameters. Therefore the variability covered by the various curves in Figure 4.4.1 does not yet represent a solid quantitative measure for the uncertainty in the $Q_{Max}(RP)$ of Lobith that was found for the reference setting of the flooding parameters (as represented by the blue curve in Figure 4.3.1). The various curves merely provide a potential range of $Q_{Max}(RP)$ variations due to uncertainties in the flooding mechanisms. It must be mentioned, however, that this “potential range” is expected to over-estimate the true range. One reason for this presumption is that the present range in the $Q_{Max}(RP)$ is found for maximal (physically realistic) variations of the flooding parameters. Secondly, the variations consisted of a simultaneous (uniform for all river sections) increase or decrease of all the guard heights and other flooding parameters. In practice such a highly spatially correlated variation is neither very realistic.

To “upgrade” the present sensitivity analysis to a more sound uncertainty analysis (all or not in combination with the uncertainties in the synthetic weather series, and the HBV-parameters in the hydrological models) probability distributions must be derived for the several flooding parameters. For a (Monte Carlo based or other representatively constructed) sample from these distributions GRADE simulations can be carried out to obtain a corresponding sample for the discharges $Q(RP)$ at Lobith. From this sample the spread, a confidence interval, or other measures for the uncertainty in the $Q(RP)$ can then be derived. The estimate for the uncertainty will be more realistic than the ‘uncertainty range’ depicted in Figure 4.4.1. At this moment we do not speculate about the magnitude of this flooding induced uncertainty.

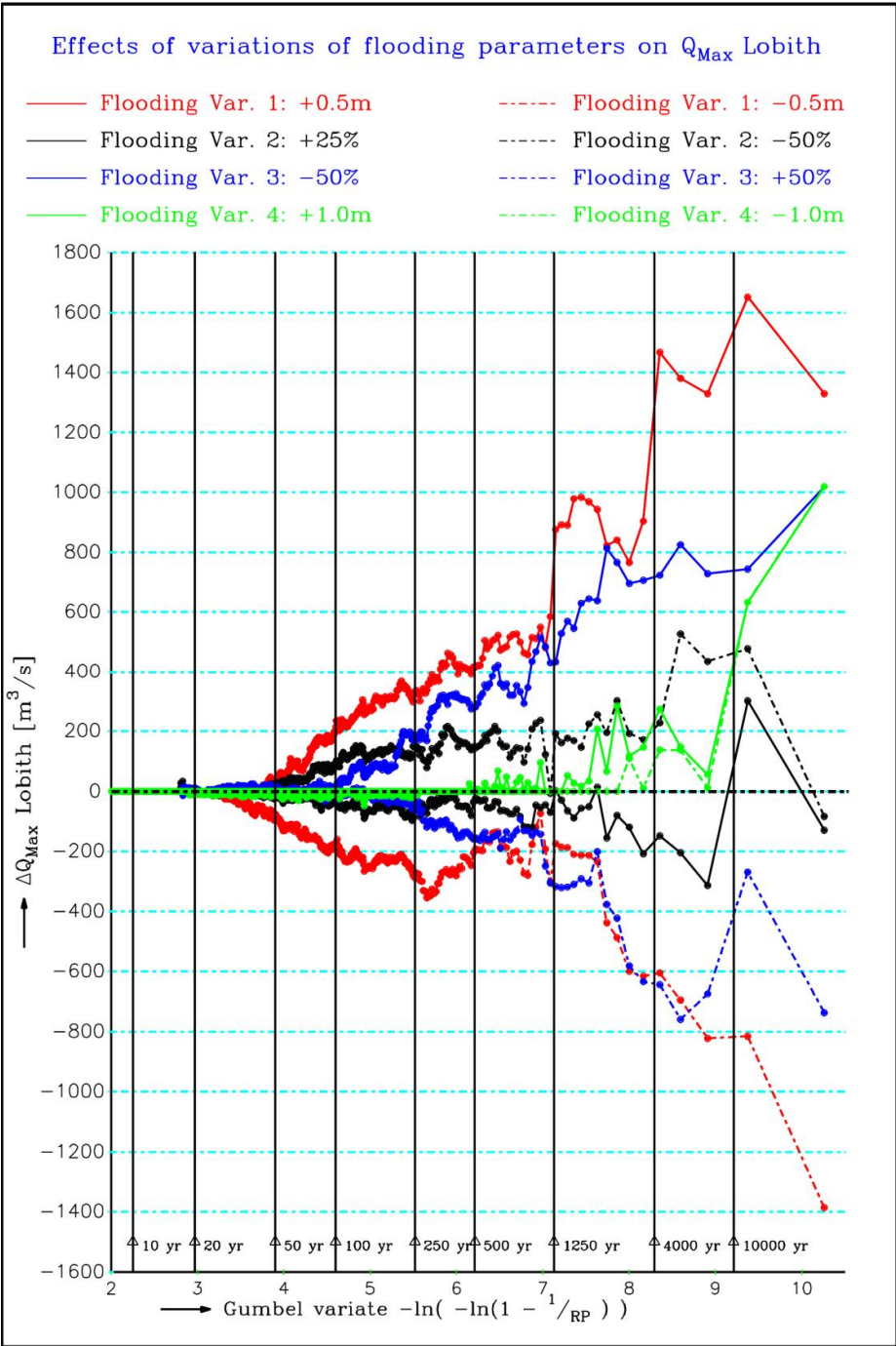


Figure 4.4.1 Effect of variations of flooding parameters on the frequency curve of annual extreme discharges for the Rhine at Lobith. The effect ΔQ_{Max} of a variation of a flooding parameter is shown here with respect to the Q_{Max} that is found with the reference setting of the flooding parameters. A positive ΔQ_{Max} means that the variation of the flooding parameter induces an increase of the Q_{Max} at Lobith

5 GRADE uncertainty analysis for discharge extremes for the Meuse at Borgharen

The uncertainty analysis of Grade for the Meuse is similar in nature to that of GRADE for the Rhine. The main differences are:

- 1 For the Meuse flooding is not included. Uncertainty estimates for extreme discharges at Borgharen are therefore derived in twofold: (i) with the discharges at Borgharen according to the hydrological HBV-models, and (ii) according to SOBEK without flooding for the Meuse.
- 2 For the Meuse a set of 24 synthetic weather series (that represents the uncertainty in the climate) are used in the uncertainty analysis (instead of a set of 11 for the Rhine).

The regression between the HBV and SOBEK annual maxima at Borgharen based on the 50,000-year reference GRADE simulation for the Meuse is presented in Appendix C. It is found that the regression based SOBEK estimates of these discharge maxima are virtually identical to the HBV computed values. For this reason it makes no sense to discriminate between these two, and in the remainder of this chapter merely the SOBEK-based results of the uncertainty analysis are shown.

Table 5.1 presents the GRADE uncertainty matrix for the discharges $Q_{Borgharen}^{Max}(RP)$ for the Meuse at Borgharen with a return period of 1250 years. Table 5.2 shows similar results for the return period of 4000 years.

For a set of return periods in the range of 5 to 10,000 years the GRADE estimates for the discharge at Borgharen and the corresponding uncertainties are presented in Table 5.3.

Table 5.1 GRADE Uncertainty Matrix for the yearly maximum discharge $Q_{Borgharen}^{Max}$ (RP) at Borgharen (Meuse) for return period RP=1250 years, according to SOBEK.

HBV ► WG ▼	5% Par. Comb.	25% Par. Comb.	50% Par. Comb.	75% Par. Comb.	95% Par. Comb.	Mean HBV (m_{HBV})	Spread HBV (s_{HBV})
WG Ref.	3654	3759	3933	3949	4050	3896	112
WG 1	3582	3649	3880	3854	3979	3815	123
WG 2	3619	3713	3941	3925	4042	3878	126
WG 3	3574	3640	3858	3864	3968	3807	123
WG 4	3433	3506	3634	3682	3747	3621	92
WG 5	3529	3590	3814	3810	3922	3759	123
WG 6	3640	3714	3962	3961	4078	3901	137
WG 7	3636	3709	3927	3927	4024	3872	120
WG 8	3602	3670	3890	3896	4017	3841	126
WG 9	3626	3682	3909	3926	4024	3860	128
WG 10	3600	3683	3889	3883	3978	3834	114
WG 11	3670	3735	3913	3943	4004	3878	105
WG 12	3737	3808	4035	4019	4123	3972	120
WG 13	3619	3686	3905	3909	4022	3854	124
WG 14	3650	3710	3893	3922	4007	3860	111
WG 15	3583	3656	3853	3870	3964	3811	116
WG 16	3652	3731	3930	3952	4046	3889	119
WG 17	3595	3699	3892	3886	4003	3842	116
WG 18	3610	3705	3921	3907	4026	3862	122
WG 19	3628	3681	3902	3895	4006	3847	120
WG 20	3593	3685	3908	3895	4020	3849	126
WG 21	3634	3705	3942	3926	4028	3876	125
WG 22	3710	3792	4036	4031	4135	3972	133
WG 23	3643	3720	3924	3930	4037	3877	119
WG 24	3707	3786	4017	4012	4128	3959	128
Mean WG (m_{WG})	3620	3694	3907	3909	4014		
Spread WG (s_{WG})	287	294	369	331	358		
Overall Mean (m): 3856 [m^3/s] Overall Standard Deviation (s): 357 [m^3/s]							
95% symmetric confidence interval $Q_{Borgharen}^{Max}$ for return period 1250 years: (3160, 4560) [m^3/s]							

Table 5.2 GRADE/SOBEK Uncertainty Matrix for the yearly maximum discharge $Q_{Borgharen}^{Max}$ (RP) at Borgharen (Meuse) for return period RP=4000 years

HBV ► WG ▼	5% Par. Comb.	25% Par. Comb.	50% Par. Comb.	75% Par. Comb.	95% Par. Comb.	Mean HBV (m_{HBV})	Spread HBV (s_{HBV})
WG Ref.	3909	4044	4218	4240	4336	4181	117
WG 1	3830	3890	4173	4096	4262	4078	139
WG 2	3845	3959	4225	4204	4325	4148	145
WG 3	3798	3858	4114	4113	4218	4050	136
WG 4	3665	3743	3881	3937	4010	3869	102
WG 5	3733	3774	4033	4009	4133	3962	132
WG 6	3898	3967	4283	4269	4375	4196	160
WG 7	3876	3969	4217	4206	4302	4148	133
WG 8	3845	3921	4175	4159	4304	4109	140
WG 9	3868	3903	4159	4194	4282	4109	142
WG 10	3815	3908	4132	4102	4188	4060	116
WG 11	3959	4027	4221	4250	4294	4178	110
WG 12	4056	4119	4391	4338	4455	4302	132
WG 13	3849	3907	4158	4160	4284	4099	138
WG 14	3900	3941	4142	4188	4282	4113	123
WG 15	3824	3890	4115	4133	4227	4066	127
WG 16	3929	4007	4228	4255	4337	4181	128
WG 17	3825	3963	4151	4130	4256	4096	116
WG 18	3863	3972	4245	4191	4338	4157	143
WG 19	3914	3937	4210	4183	4315	4136	136
WG 20	3901	4007	4235	4223	4342	4173	129
WG 21	3901	3968	4282	4225	4336	4179	149
WG 22	4002	4097	4388	4364	4473	4302	150
WG 23	3859	3934	4147	4152	4256	4097	121
WG 24	3984	4081	4334	4298	4438	4259	136
Mean WG (m_{WG})	3872	3948	4193	4183	4293		
Spread WG (s_{WG})	390	413	509	447	467		
Overall Mean (m): 4128 [m^3/s] Overall Standard Deviation (s): 477 [m^3/s]							
95% symmetric confidence interval $Q_{Borgharen}^{Max}$ for return period 4000 years: (3190, 5060) [m^3/s]							

Table 5.3 GRADE/SOBEK estimates for the annual maximum discharge $Q_{Borgharen}^{Max}(RP)$ at Borgharen (Meuse) and its uncertainty for a set of return periods in the range of 5 to 10,000 years. The listed discharges and uncertainty measures have been rounded off to the nearest multiple of 10.

Return Period [years]	Estimate of $Q_{Borgharen}^{Max}(RP)$ [m^3/s]	Spread in $Q_{Borgharen}^{Max}(RP)$ [m^3/s]	Symmetric 95% confidence interval for $Q_{Borgharen}^{Max}(RP)$ [m^3/s]	
			Lower Bound	Upper Bound
5	1960	120	1730	2190
10	2290	150	2010	2580
20	2600	210	2190	3020
50	2970	280	2430	3510
100	3210	290	2640	3790
250	3480	290	2910	4050
500	3640	300	3060	4230
1250	3860	360	3160	4560
4000	4130	480	3190	5060
10000	4340	590	3190	5500

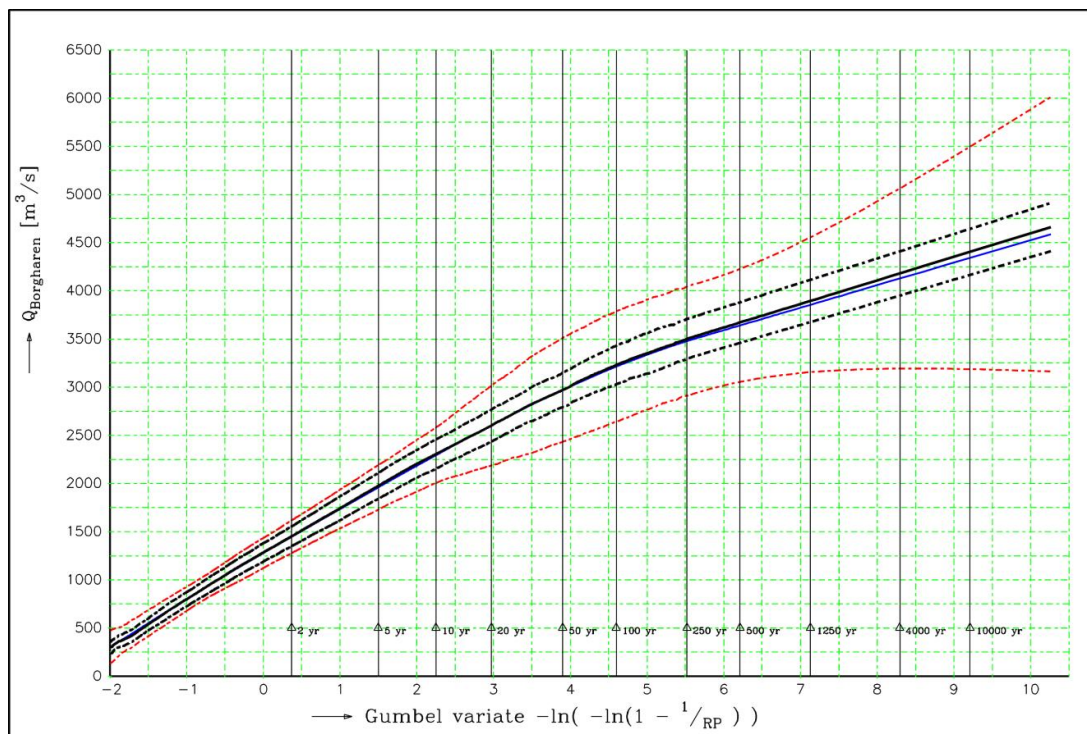


Figure 5.1 Frequency curve for extreme discharges of the Meuse at Borgharen, according to GRADE/SOBEK. The solid curve in blue represents the estimate of $Q(RP)$ for the various return periods RP . The lower and upper bounds of the 95% confidence in this estimate are denoted by the red coloured dashed curves. In the computation of these $Q(RP)$ and confidence intervals the uncertainty in the climate and in the HBV-models are both taken into account. The curves in black represent the $Q(RP)$ and its confidence intervals for the uncertainty in the HBV-models only

As for the Rhine, the tables with the uncertainty matrices and Figure 5.1 show that also for the Meuse the uncertainties in the estimates for the $Q_{Borgharen}^{Max}$ are highly dominated by the uncertainty in the climate. For example, for $RP=1250$ year the average of the spreads listed in the last row of the uncertainty matrix (forming an averaged weather climate induced uncertainty) is about $330 \text{ m}^3/\text{s}$ and is about 2.7 times as large as the average $120 \text{ m}^3/\text{s}$ of the spreads listed in the last column (forming an averaged HBV induced uncertainty). For $RP=4000$ year this ratio of the spreads increases to 3.4.

The tables and Figure 5.1 also indicate that for the longer return periods the total uncertainty in the $Q_{Borgharen}^{Max}(RP)$ increases more than proportionally with the return period RP than $Q_{Borgharen}^{Max}(RP)$ does. In fact, for $RP=1250$ year the spread is 9.3% of $Q_{Borgharen}^{Max}(RP)$ while for $RP=4000$ and $RP=10,000$ year this ratio is 11.6% and 13.6%.

For the Rhine these ratios of the spread and $Q_{Lobith}^{Max}(RP)$ were 6.6%, 7.8% and 8.8% respectively. This suggests a relatively larger amount of uncertainty in the (GRADE estimates of) extreme discharges for the Meuse than for the Rhine.

From the entries in the uncertainty matrices listed above it can also be recognised that for the Meuse the computed discharges tend to increase much more monotonically along the rows (i.e. for the five HBV-parameter combinations) than was found for the Rhine (see Section 4.1). The reason of 'better' monotonic dependency on the HBV-parameter sets is probably that within the GLUE calibration procedure for the Meuse the selection of the HBV-parameter combinations was based on extreme discharges for just the one Meuse sub-basin. Moreover the extreme discharges within this selection were for a substantially longer return period (100 year) than for the Rhine (10 year).

6 Final GRADE discharge frequency curves and uncertainties for Lobith and Borgharen

Within the present scope (with GRADE brought into the WTI² project) estimates and uncertainties for extreme discharges at Lobith and Borgharen are desired for return periods up to (at least) 50,000 year. In the uncertainty analyses of Chapter 4 and 5 for the Rhine and Meuse GRADE simulations were carried out of length 20,000 year, however. The main reason for using this shorter length within in the uncertainty analysis is the much longer computation time that would be required when for all the 11×5 (Rhine) and 24×5 (Meuse) combinations of synthetic weather series and HBV-parameter sets GRADE simulations of length 50,000 years had to be carried out.

In the present work computations of length 50,000 years were limited to a GRADE 'reference simulation only. In this simulation the reference synthetic weather series is combined with the 50% HBV parameter set. The SOBEK based results of the reference simulation are then used to derive the 'final' estimates of extreme discharges and discharge frequency curves at Lobith and Borgharen for return periods up to 50,000 year or even longer using Weissman's method for extrapolation (see Section A.3 in Appendix A).

For the Rhine this is done in twofold: for the SOBEK model without flooding, and for a SOBEK model in which flooding is also included.

The simulations within the uncertainty analyses of Chapter 4 and 5 are used to obtain the uncertainties in these 'final' estimates. For return periods up to about 20,000 years the uncertainties are 'merely' copied. For higher return periods the uncertainties are derived by means of extrapolation, using again Weissman's method.

The frequency curve for the extreme discharges (together with the uncertainty in the form of the lower and upper bound of a 95% confidence interval) of the Rhine at Lobith are shown below in the Figures 6.1a (SOBEK without flooding) and 6.1b (SOBEK with flooding).

For the Meuse at Borgharen the 'final' frequency curve (without flooding) is presented in Figure 6.2.

These figures are to a large extent similar to the frequency plots already presented in Chapters 4 and 5. The main difference is that now the estimate of a frequency curve is based on the reference GRADE simulations of length 50,000 years, rather than a (weighted) mean over an ensemble of 11×5 (Rhine) or 24×5 (Meuse) joint variations of the weather climate and HBV-parameter sets. The uncertainty bands derived in the uncertainty analysis have been placed symmetrically around the frequency curve derived from the 50,000 years reference simulations.

In the Tables 6.1ab en 6.2 these 'final' GRADE estimates and uncertainties of the annual maximum discharge are also listed in a more quantitative form for a set of representative return periods within the range of 2 to 100.000 year.

² WTI stands for "Wettelijk Toets Instrumentarium". WTI is the Dutch method for analyzing dikes along the Dutch primary and secondary flood defense structures. Within WTI discharge frequency curves are desired for the Rhine at Lobith and the Meuse at Borgharen for return periods up to at least 50,000 years or even 100,000 years. For these discharges the uncertainty in the form of a 95% confidence interval are also required.

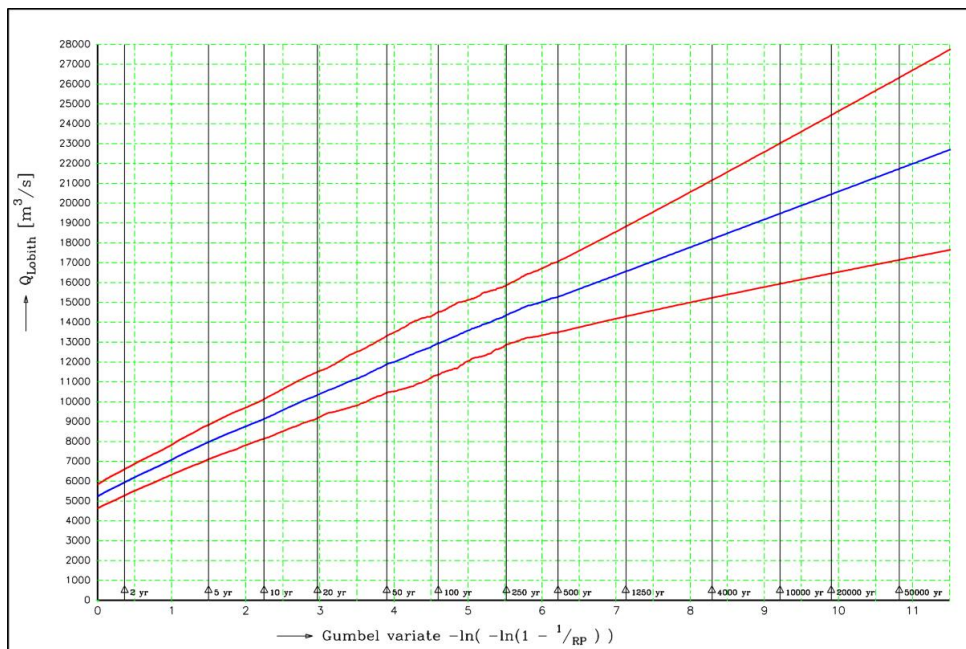


Figure 6.1a Frequency curve and uncertainties for extreme discharges of the Rhine at Lobith according to GRADE. The solid curve in blue represents the frequency curve derived from the GRADE reference simulation of length 50,000 years, using a SOBEK model where effects of flooding are not included. The red curves denote the lower and upper bound of the 95% confidence interval as derived in the uncertainty analysis

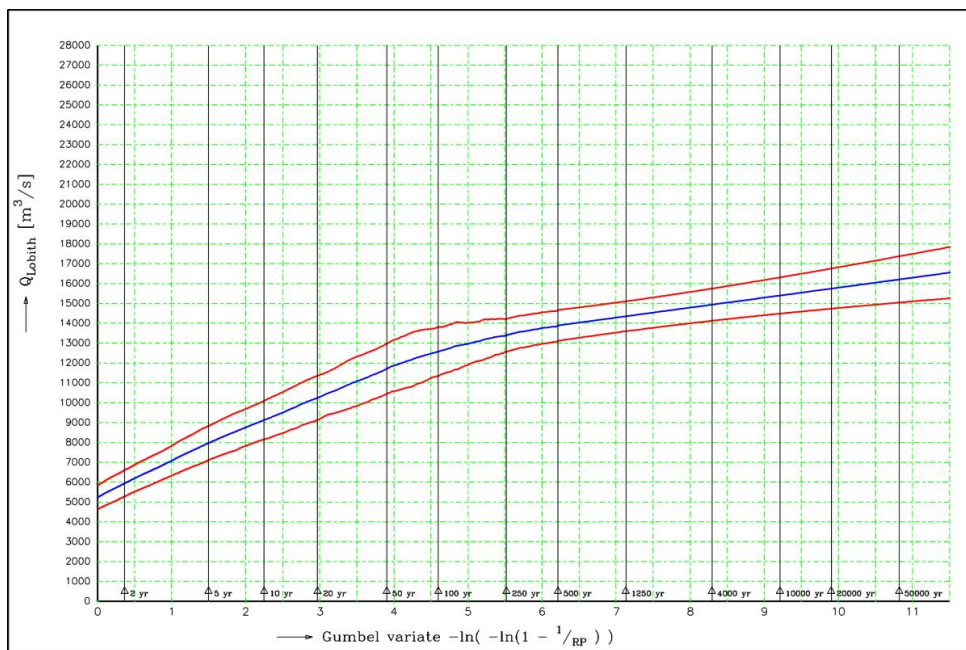


Figure 6.1b Frequency curve and uncertainties for extreme discharges of the Rhine at Lobith according to GRADE. The solid curve in blue represents the frequency curve derived from the GRADE reference simulation of length 50,000 years, using a SOBEK model where effects of flooding are also included. The red curves denote the lower and upper bound of the 95% confidence interval as derived in the uncertainty analysis

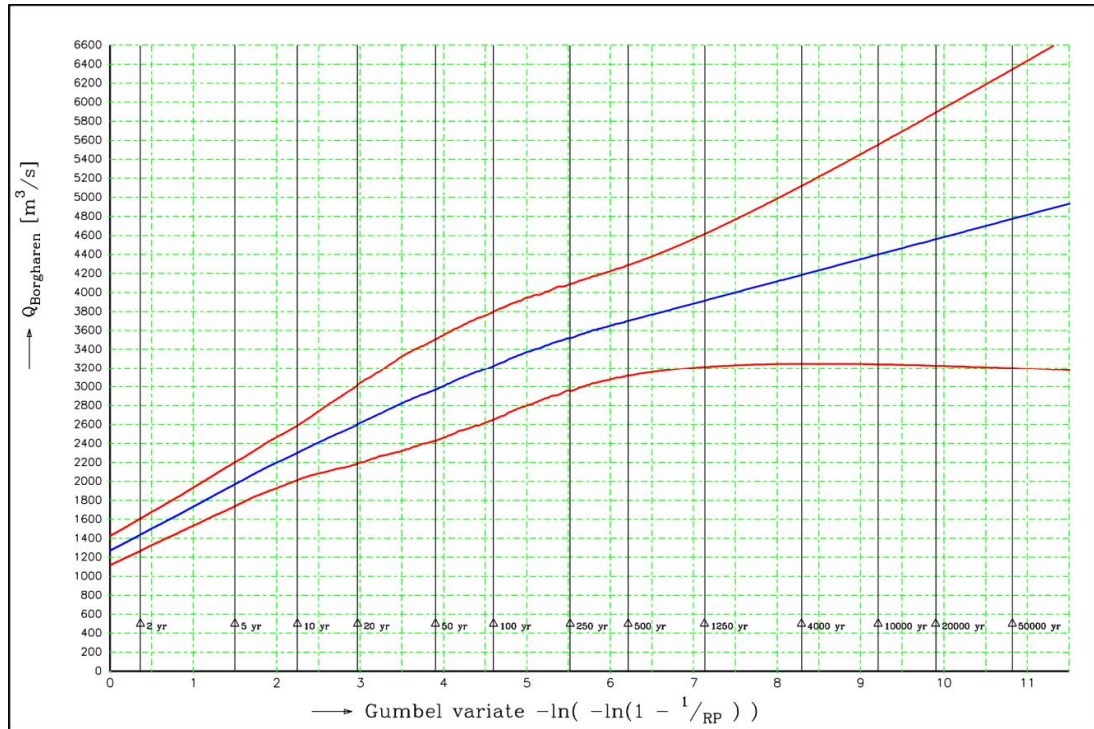


Figure 6.2 Frequency curve and uncertainties for extreme discharges of the Meuse at Borgharen according to GRADE. The solid curve in blue represents the frequency curve derived from the GRADE reference simulation of length 50,000 years, using a SOBEK model (without flooding). The red curves denote the lower and upper bound of the 95% confidence interval as derived in the uncertainty analysis

Table 6.1a GRADE estimates for the annual maximum discharge $Q_{Lobith}^{Max}(RP)$ at Lobith (Rhine) and its uncertainty for a set of representative return periods in the range of 2 to 100,000 years, based on the SOBEK-model without flooding. The listed discharges and uncertainty measures have been rounded off to the nearest multiple of 10

Return Period [years]	Estimate of $Q_{Lobith}^{Max}(RP)$ [m^3/s]	Spread in $Q_{Lobith}^{Max}(RP)$ [m^3/s]	Symmetric 95% confidence interval for $Q_{Lobith}^{Max}(RP)$ [m^3/s]	
			Lower Bound	Upper Bound
2	5940	340	5280	6610
5	7970	440	7100	8840
10	9140	510	8140	10140
20	10340	590	9180	11510
50	11890	730	10460	13320
100	12940	810	11350	14530
250	14380	760	12890	15880
500	15270	910	13490	17060
1,250	16560	1160	14300	18830
2,000	17220	1300	14680	19760
4,000	18190	1510	15230	21150
10,000	19480	1810	15940	23020
20,000	20450	2030	16460	24440
50,000	21740	2340	17140	26330
100,000	22710	2580	17660	27760

Table 6.1b GRADE estimates for the annual maximum discharge $Q_{Lobith}^{Max}(RP)$ at Lobith (Rhine) and its uncertainty for a set of representative return periods in the range of 2 to 100,000 years, based on the SOBEK-model with flooding. The listed discharges and uncertainty measures have been rounded off to the nearest multiple of 10

Return Period [years]	Estimate of $Q_{Lobith}^{Max}(RP)$ [m^3/s]	Spread in $Q_{Lobith}^{Max}(RP)$ [m^3/s]	Symmetric 95% confidence interval for $Q_{Lobith}^{Max}(RP)$ [m^3/s]	
			Lower Bound	Upper Bound
2	5940	340	5280	6600
5	7970	440	7110	8830
10	9130	500	8150	10110
20	10250	570	9140	11360
50	11710	640	10440	12970
100	12580	630	11350	13810
250	13390	420	12570	14220
500	13890	400	13110	14670
1,250	14350	390	13600	15110
2,000	14590	390	13820	15360
4,000	14940	410	14130	15750
10,000	15400	470	14490	16310
20,000	15750	520	14740	16760
50,000	16210	590	15050	17380
100,000	16560	660	15270	17850

Table 6.2 GRADE estimates for the annual maximum discharge $Q_{Borgharen}^{Max}(RP)$ at Borgharen (Meuse) and its uncertainty for a set of representative return periods in the range of 2 to 100,000 years, based on a SOBEK-model without flooding. The listed discharges and uncertainty measures have been rounded off to the nearest multiple of 10

Return Period [years]	Estimate of $Q_{Borgharen}^{Max}(RP)$ [m^3/s]	Spread in $Q_{Borgharen}^{Max}(RP)$ [m^3/s]	Symmetric 95% confidence interval for $Q_{Borgharen}^{Max}(RP)$ [m^3/s]	
			Lower Bound	Upper Bound
2	1440	90	1270	1610
3	1690	100	1490	1880
4	1850	110	1640	2070
5	1970	120	1740	2200
10	2300	150	2010	2590
20	2600	210	2190	3020
50	2970	280	2430	3510
100	3220	290	2650	3800
250	3520	290	2950	4090
500	3700	300	3110	4290
1,250	3910	360	3210	4610
2,000	4020	400	3240	4810
4,000	4180	480	3250	5120
10,000	4400	590	3240	5550
20,000	4560	680	3230	5890
50,000	4770	800	3200	6350
100,000	4930	900	3180	6690

7 Summary and conclusions

7.1 Summary

The main issue in this report is an uncertainty estimation of the extreme discharges computed by GRADE. In the present report these events refer to annual discharge maxima at Lobith (at the downstream reach of the Rhine) and Borgharen (downstream location of the Meuse). The focus is on the estimation of the uncertainties in discharge frequency curves for these two locations.

The uncertainties in the frequency curves are derived from uncertainties that have been assigned to GRADE's model components.

One source of uncertainty in GRADE is the uncertainty in the climate, expressed by a set of different 20,000-year Weather Generator (WG) simulations. For the Rhine this set consists of 11 WG simulations and for the Meuse of 24 WG simulations. The ensemble serves as an empirical distribution of the uncertainty in the current climate (rainfall and temperature series), and in this way provides a quantitative representation of the uncertainty in the input of the hydrological models in GRADE.

The hydrological models in GRADE are another source of uncertainty. This uncertainty is limited to HBV model parameters. The uncertainties in these HBV-parameters have been identified within the calibration using a GLUE analysis. To keep computation times in the uncertainty analysis to a practically manageable amount the set of all behavioural parameter combinations had to be reduced. For both the Meuse basin and the major sub-basins of the Rhine five representative HBV parameter sets were selected from the 5%, 25%, 50%, 75% and 95% quantiles of the computed 10-year (Rhine) or 100-year (Meuse) discharges for a large number of behavioural HBV-parameter combinations. These five HBV-parameter sets then finally represent an empirical distribution for the uncertainty in the hydrological models. As a matter of their construction these five sets are not equally likely. Therefore a weight or probability was derived for each of these sets.

Uncertainties will also be present in the hydrodynamic SOBEK models within GRADE (as a third component in a GRADE system). This holds for the SOBEK models without flooding, but particularly for the SOBEK version in which additionally the effects of flooding are also modelled. On entry to the present work no analysis or quantitative estimates for these uncertainties were available. For this reason uncertainties in the hydrodynamic models within GRADE have not been considered. This will not be a serious omission since the uncertainty in the hydrodynamic models is expected to be substantially smaller than those in the hydrological models. If flooding and dike breaks are included in the SOBEK models this remains to be verified, however.

As a result the (total) uncertainty in GRADE is represented by a combination of two empirical distributions. Schematically this is depicted with an "Uncertainty Matrix". For the estimation of uncertainties in GRADE estimates, 20,000-year GRADE simulations are performed for every entry of the uncertainty matrix. Appendix A describes how from this uncertainty matrix the uncertainty estimates of GRADE results can be derived.

This uncertainty analysis has been applied to derive the uncertainties in the GRADE estimates of discharge frequency curves for Lobith (Rhine) and Borgharen (Meuse). In this analysis several alternatives have been discriminated. For example:

1. The frequency curves and their uncertainties according to solely the hydrological model.
2. Comparison of the amount that the uncertainties in the individual GRADE-components (the model input, and the hydrological HBV models) contribute to the overall uncertainty in the discharge frequency curves.
3. Comparison of frequency curves and uncertainties according to HBV and those according to SOBEK using the model where effects of upstream flooding and/or overflows are ignored.
4. The frequency curves and their uncertainties using a version of SOBEK in which also flooding is taken into account.

The main conclusions are summarized below.

Within the uncertainty analysis a number of assumptions, simplifications, approximations, “short cuts”, etc. have been made. These, and other limitations that leave space for further improvements, are discussed in Chapter 8

7.2 Conclusions

The uncertainty in the discharge frequency curves for both the Rhine and Meuse is highly dominated by the uncertainty in the climate (as represented by the set of different WG simulations). No uncertainties of the SOBEK-models have been taken into account. It is therefore uncertain whether uncertainties in the SOBEK model will ‘significantly’ affect the total uncertainty. Particularly parameters that relate to flooding might substantially contribute to the uncertainties.

The results for the Rhine at Lobith reveal a strong effect of flooding on the discharge frequency curves (for the most extreme discharges). For GRADE this emphasizes the importance of including and improving flooding mechanisms in the hydrodynamic SOBEK models.

For the uncertainty bands a large effect of flooding is observed as well. This effect is in the form of a much smaller width compared to the situation that flooding is not modelled. Uncertainties in the flooding parameters may again increase the width of the confidence intervals, however. No uncertainty analysis was carried out to quantify this effect. A sensitivity analysis, however, revealed considerable effects for some flooding parameters (as for example dike heights).

In relative sense the uncertainty in the GRADE estimates of extreme discharges tend to be larger for the Meuse (Borgharen) than for the Rhine (Lobith). Here this was established through the ratio $\sigma[Q(RP)]/Q(RP)$ of the spread in – and the estimate of an extreme discharge $Q(RP)$ for a given return period RP .

At the same time for both cases the ratio $\sigma[Q(RP)]/Q(RP)$ tends to increase with the return period RP , suggesting that the uncertainty increases more with RP than $Q(RP)$ does.

8 Remarks, discussion and further developments

Number of WG simulations representing the climate uncertainty

To represent the uncertainties in the climate a jackknife ensemble was constructed. The size of this ensemble is relatively small: 11 members for the Rhine and 24 members for the Meuse. Because of this relatively small size the estimates, in particular for the Rhine, the uncertainty estimates for extreme discharges have a relatively large standard error. This standard error can be reduced by using a smaller block size in the jackknife procedure (for the Meuse the block size used is three years and for the Rhine it is five years). Reducing the block size leads to a larger sample size, and consequently to a substantial increase of computation time.

Alternative combinations of the HBV-parameter sets

The uncertainty in the HBV models of the Rhine basin was represented by 5 parameter combinations. These consisted of “quantile wise combinations” (5, 25, 50, 75, 95%) of the parameter sets for each of the 15 major sub-basins. This form of combination assumes full mutual dependency of the parameter sets of the major sub-basins. To obtain an impression of the effect of this assumption, the “opposite” situation of fully mutually independent parameter sets can be considered. A proper recipe must then be found to select a practically treatable number of representatives (again 5, for example) out of all 5^{15} feasible combinations and the uncertainty analysis should be repeated. It is expected that the outcome of this second uncertainty analysis will differ only slightly from the present results.

For the Meuse the five representative HBV parameter-combinations were based on simulated once in hundred year discharges at Borgharen while for the Rhine a return period of ten years was used. This shorter period may be a reason that for the Rhine the discharges depend less monotonically on the HBV-parameter sets than for the Meuse.

Skew confidence intervals

Uncertainties in the discharge frequency curves have been derived by means of a standard error. Assuming a Gaussian distribution for the estimates of extreme discharges, this standard error is used for the computation of the lower and upper bound of a (95%) confidence interval. This yields a symmetric confidence interval, and skewness in the distribution of quantiles is ignored. Skewness may be present, however, for the high(er) discharges (or equivalently: the higher return periods) and may particularly become large when effects of flooding and overflows become notable. In that case the discharge will be bound from above. This induces a skew distribution, and the necessity of generating skew confidence intervals. In the present case we could not do much better than producing symmetric confidence intervals because of the rather small amount of variations in the representation of the uncertainties in the weather climate and the HBV models.

SOBEK evaluations of the uncertainty matrix

In the present case SOBEK computations of extreme discharges were only carried out for the reference situation. The SOBEK estimates for annual discharge extremes (at Lobith and Borgharen) correlate reasonably well with the ones computed by HBV. A high correlation was particularly found for the largest extremes (and thus highest return periods). This SOBEK-HBV correlation was used to derive a regression formula for translating HBV computed discharge extremes to corresponding SOBEK estimates. To save computation time these regressions were then used for the uncertainty analysis. No uncertainty in the regression formulae was taken into account.

This uncertainty is not fully negligible as can be recognised from SOBEK versus HBV scatter plots. Therefore the presently derived uncertainties in the SOBEK-based frequency curves may be under estimated. It is expected that the uncertainty induced by the regression is limited.

Underestimates of the uncertainties in the HBV models

The uncertainty in the hydrological models has been represented by means of a set of model parameters. Apart from these parameters no other model uncertainties (e.g. conceptual or structural uncertainties) have been taken into account. These uncertainties are likely to be larger for discharge extremes. See e.g. the results of a validation of the HBV models for the Meuse presented by Kramer and Schroevers (2008). This suggests taking structural uncertainties into account as well. Quantitative estimates for this type of uncertainty may be obtained through (stochastic) output correction models. The idea is, for example, to identify a suitable parameterised, and relatively simple regression model to relate HBV computed discharge extremes to correspondingly observed extremes (similarly as done here in Appendix B to convert HBV computed discharges to corresponding SOBEK values). The formula can then be applied to the HBV discharges computed within the GRADE uncertainty analysis (provided the formula makes also sense for higher discharges than the observed). By means of this regression model any systematic errors in the HBV computed discharge extremes can be reduced and also a quantitative measure for their uncertainty derived. As a result the total uncertainty in GRADE predictions of extreme discharges may increase, and at the same time be more representative. Apart from the expected increase, the total uncertainty will to a higher extent be determined by the HBV models instead of being fully dominated by the uncertainty in the climate.

Uncertainties in the hydrodynamic models

In the present study uncertainties in the hydrodynamic SOBEK models of the Rhine and Meuse have been ignored. For flow conditions without flooding and overflows this is presumably not a serious omission since for such conditions the uncertainty in the SOBEK model tends to be negligible compared to the uncertainties in the other GRADE components. In a sensitivity analysis of the SOBEK-model for the Rhine relatively large effects of parameters in the flooding mechanisms were found³. As a result uncertainties in these parameters may also increase the uncertainty in GRADE estimates. The amount of this increase, and how it compares to the contributions of the other GRADE components, is still unknown and should be further investigated.

³ Note that in the sensitivity analysis the parameter changes were applied for all flooding locations in the model at once.

9 Literature

Beersma, J.J., T.A. Buishand, T.A., and Wójcik, R: Weather generator for the Rhine basin: multisite simulation of daily weather variables by nearest-neighbor resampling. In: Generation of hydrometeorological reference conditions for the assessment of flood hazard in large river basins (P. Krahe and D. Herpertz. Eds.), 69-77. CHR, Report 1-20, 2001.

Beven, K. J., Binley, A. M.: The future of distributed models: model calibration and uncertainty prediction, *Hydrol. Proc.*, 6, 279–298, 1992.

Boos, D.D.: Using extreme value theory to estimate large percentiles. *Technometrics*, Vol. 26, pp. 33-39, 1984.

Buishand, T.A., Brandsma, T.: Multisite simulation of daily precipitation and temperature in the Rhine basin by nearest neighbor resampling. *Water Resources Research*, 37, 2761-2776, 2001.

Buishand, T.A., Leander, R.: Weather generator for the Meuse basin: Extension of the base period with the years 1999-2008. Publication 196-V, KNMI, De Bilt, 2011.

Davison, A.C., Hinkley, D.V.: *Bootstrap Methods and their Application*. Cambridge University Press, 1997.

Efron. B., Tibshirani, R.J.: *An introduction to the bootstrap*. Chapman & Hall, 1993

Hegnauer, M, van Verseveld, W.: Generalised Likelihood Uncertainty Estimation for the daily HBV model in the Rhine Basin, Part B: Switzerland. Report 1207771-003-ZWS-0017, Deltares, 2013.

IKSR: Nachweis der Wirksamkeit von Maßnahmen zur Minderung der Hochwasserstände im Rhein, Umsetzung des Aktionsplans Hochwasser 1995 – 2010 einschließlich Vorausschau für 2020 sowie 2020+, Internationale Kommission zum Schutz des Rheins. Report 199, ISBN 3-941994-18-2978-3-941994-18-8 (available in German, Dutch and French), 2012.

Kramer, N., Beckers, J., and Weerts, A.: Reliability of the Generator of Rainfall and Discharge Extremes (GRADE), Parts D & E, Report Q4424, Deltares, June 2008.

Kramer, N., Schroevers, R.: Generator of Rainfall and Discharge Extremes (GRADE), Part F. Report Q4424, Deltares, December 2008.

Lammersen, R.: Effects of extreme floods along the Niederrhein (Lower Rhine), final report (in German ISBN 9036956382, in Dutch ISBN 9036956390). Landwirtschaft und Verbraucherschutz des Landes Nordrhein–Westfalen, Düsseldorf, Germany; Provincie Gelderland, Arnhem, The Netherlands; Rijkswaterstaat Directie-Oost, Arnhem, The Netherlands, 2004.

Leander, R., T.A. Buishand, T.A., Aalders P., and De Wit, M: Estimation of extreme floods of the Meuse using a stochastic weather generator and a rainfall-runoff model. *Hydrological Sciences Journal*, 50(6), December 2005.

Meijer, D.G.: Aktualisierung des SOBEK-Modells Iffezheim/Maxau – Andernach Erstellung der BASELINE-Datensätze und der SOBEK-Modelle, hydraulische und morphologische Modellkalibrierung und – Verifizierung. Bundesanstalt für Gewässerkunde, November 2009.

Ogink, H.J.M.: Design discharge and design hydrograph computation for Meuse and Rhine rivers. Comparison of computational methods. August 2012.

Schmeits, M., Wolters, L.A., Beersma, J.J., and Buishand, T.A.: Weather generator for the Rhine basin: Description of simulations using gridded precipitation datasets and uncertainty analysis. Publication 186-VII, KNMI, De Bilt, 2014a.

Schmeits, M., Beersma, J.J., and Buishand, T.A.: Weather generator for the Meuse basin: Description of simulations with and without a memory term and uncertainty analysis. Publication 196-VI, KNMI, De Bilt, 2014b.

Udo, J. and Termes, P.: Gevoeligheidsanalyse hydraulica met GRADE. Bepalen variatie dijkoverstromingsparameters. Report PR2479.30 (in Dutch), HKV Lijn in Water, October 2013.

Vieira da Silva, J., Barneveld, H.J., and Wijbenga, J.H.A.: Grade. Dijkoverstroming Niederrhein: SOBEK versus WAQUA. Report PR2479_20_02, HKV Lijn in Water, March 2013.

Weissman, I: "Estimation of parameters and larger quantiles based on the k largest observations", Journal of the American Statistical Association, Vol. 73, No. 364, pp. 812–815, 1978.

Winsemius, H., Van Verseveld, W., Weerts, A., and Hegnauer, M.: Generalised Likelihood Uncertainty Estimation for the daily HBV model in the Rhine Basin. Part A: Germany. Report 1207771-003-ZWS-0018, 2013.

A Description of the GRADE uncertainty analysis method

In Chapter 2 the representation of the uncertainties in the main GRADE components has been outlined. In this appendix the procedure is described how the uncertainties within the components are combined to obtain the 'total' uncertainty in GRADE based estimates of extreme discharges.

A.1 The uncertainty matrix

As described in Section 2.1 the uncertainty in the current weather climate is represented by an ensemble of rainfall and temperature time series. For the Rhine this has led to an ensemble of 11 synthetic rainfall and temperature time series, each of length 20,000 years. These 11 feasible realizations provide an empirical distribution for the variability and within GRADE thus the uncertainty in the weather climate. The same holds for the Meuse, but here the ensemble size of synthetic weather series is 24.

As a matter of the procedure sketched in Section 2.2 the uncertainty in the hydrological (rainfall) modeling is represented by an empirical distribution as well. For both the Rhine and the Meuse this ensemble consists of 5 sets of combinations of uncertain parameters in the HBV-models of the several sub-basins.

The 'overall' uncertainty in GRADE is then represented by the mutual combinations of the elements of these two (rainfall and HBV-parameter) ensembles. For the Rhine this is illustrated by the matrix depicted below in Table A.1.1 (NB: This table is identical to Table 3.1.1). The 5 variations of the HBV parameters are arranged along the columns, while the variations for the weather climate are arranged along the rows. In the (*i*-th row, *j*-th column) entries of the matrix a 'target' variable $Q(i,j)$ is listed. This target Q is the value of some quantity derived from GRADE's output when the system is run with the weather series of the *i*-th row and at the same time with the HBV-model parameters that belong to the *j*-th column. In the present approach, the target variables $Q(i,j)$ are the estimate for the yearly maximum discharge at Lobith that belongs to a given return period (e.g. 1250 or 4000 year).

To obtain the entries $Q(i,j)$ in the matrix of Table A.1.1 the GRADE system must be run 11×5 times. In this way an ensemble of 55 estimates for the target Q is obtained and from this ensemble an 'overall' estimate for Q has to be produced and also a measure for the uncertainty in this estimate. In the next sections the procedure to get these estimates will be described.

For the Meuse a similar reasoning holds, of course, as given above for the Rhine. For the Meuse the number of columns is also 5 but the number of rows in the matrix is then 24.

In the remainder a matrix as depicted in Table A.1.1 will be referred to as an "Uncertainty Matrix" or briefly "UM".

Finally it is mentioned that apart from the (11 or 24) Jackknife variations the GRADE system has also been run for the additional case where all observed weather data were used as basis set in the weather generator to generate synthetic rainfall/temperature series of length 20,000 year. These series, and more generally the corresponding GRADE predictions of the target variables (again for the 5 HBV-parameter combinations), will be called the "reference" situation.

Formally this reference (“WG 0”, where WG stands for “Weather Generator”) is with respect to the system’s external forcing. In a similar way the 50% HBV-parameter combination (and the GRADE’s response to the external forcing variations) can be considered as reference for the HBV-model uncertainty.

Table A.1.1 Illustration of a GRADE uncertainty matrix

HBV ► External Forcing ▼	Par. Comb 5%	Par. Comb 25%	Par. Comb 50%	Par. Comb 75%	Par. Comb 95%
WG 1	Q(1,1)	Q(1,2)	Q(1,3)	Q(1,4)	Q(1,5)
WG 2	Q(2,1)	Q(2,2)	Q(2,3)	Q(2,4)	Q(2,5)
WG 3	Q(3,1)	Q(3,2)	Q(3,3)	Q(3,4)	Q(3,5)
WG 4	Q(4,1)	Q(4,2)	Q(4,3)	Q(4,4)	Q(4,5)
WG 5	Q(5,1)	Q(5,2)	Q(5,3)	Q(5,4)	Q(5,5)
WG 6	Q(6,1)	Q(6,2)	Q(6,3)	Q(6,4)	Q(6,5)
WG 7	Q(7,1)	Q(7,2)	Q(7,3)	Q(7,4)	Q(7,5)
WG 8	Q(8,1)	Q(8,2)	Q(8,3)	Q(8,4)	Q(8,5)
WG 9	Q(9,1)	Q(9,2)	Q(9,3)	Q(9,4)	Q(9,5)
WG 10	Q(10,1)	Q(10,2)	Q(10,3)	Q(10,4)	Q(10,5)
WG 11	Q(11,1)	Q(11,2)	Q(11,3)	Q(11,4)	Q(11,5)

A.2 Computation of the uncertainty matrix

For every entry (i,j) in the uncertainty matrix a GRADE model evaluation is required. In the present case this involves a GRADE simulation over a time period of 20,000 years. The Q(i,j) will be the maximum discharge of the Rhine at Lobith (or at Borgharen for the Meuse) that corresponds to a given return period RP. For discharge frequency curves the maximum yearly discharge (and its uncertainty) must be derived for all ‘feasible’ return periods (but less than 20,000 years as a matter of the simulation time period). In this way the uncertainty matrix must be produced in multiple rather than merely once. Computation of the Uncertainty Matrix for more than one RP does not demand additional GRADE computations, however.

Due to practical limitations it was not possible to run SOBEK for all entries of the uncertainty matrix and a short cut was constructed to obtain convenient substitutes for these entries. In fact, first HBV and next SOBEK simulations were carried out for a “reference” combination of the model forcing on one hand and the HBV-parameters on the other. In these reference runs the model forcing consists of the synthetic rainfall and temperature that is produced by the weather generator when all available historic weather data is used as basis set in the resampling algorithm. For the HBV model parameters the 50% combination serves as reference. From the results of the HBV and SOBEK reference simulations for a period of 50,000 years the set of corresponding annual extreme discharges $\left\{ \left(Q_k^{Max, HBV}, Q_k^{Max, SOBEK} \right) \right\}_{k=1}^{50000}$ was selected. By means of standard scatterplots the relation between these two extreme discharges was visually inspected. Despite some scatter these plots revealed a clear and monotonic relation of the $Q^{Max, HBV}$ and $Q^{Max, SOBEK}$. This suggests that the $Q^{Max, SOBEK}$ can reasonably well be derived from the $Q^{Max, HBV}$. For this purpose a parameterised formula $f(\cdot | \Theta)$ was identified to “predict” the $Q^{Max, SOBEK}$ from the $Q^{Max, HBV}$.

The Θ denotes a set of parameters in $f(\cdot|\Theta)$ for which an estimate $\hat{\Theta}$ must be obtained such that $f(Q^{Max,HBV}|\hat{\Theta})$ match the $Q^{Max,HBV}$ as good as possible.

For the Rhine such a formula $f(\cdot|\Theta)$ was derived in twofold: first for the case that the $Q^{Max,SOBEK}$ of Lobith were computed with SOBEK without facilities for flooding, and secondly for the $Q^{Max,SOBEK}$ according to the SOBEK model in which effects of flooding were included. For the Meuse flooding was not taken into account and as a result only one such formula $f(\cdot|\Theta)$ was identified.

The calibrated functions $f(\cdot|\hat{\Theta})$ were then applied to all entries of the HBV based uncertainty matrix to obtain an approximation of the uncertainty matrix according to SOBEK.

The functions $f(\cdot|\hat{\Theta})$ that were presently identified for the HBV to SOBEK conversion of Lobith and Borgharen extreme discharges are described in Appendix B.

A.3 Variance reduction using Weissman's method

In the present uncertainty analysis the entries in the Uncertainty Matrix will be yearly maximum discharges that correspond to a given return period RP . These yearly maxima are selected from discharge time series produced by GRADE. The length of these time series is 20,000 years and with temporal resolution $\Delta t = 1$ day. Such a time series is produced for every combination of the i -th synthetic rainfall sequence and the j -th set of the HBV-parameters. From these separate time series the yearly maxima are extracted and sorted in ascending order. This yields a series $Q_{(k)}^{Max}$ for $k = 1, 2, 3, \dots, 20000$. The notation (k) means the k -th value after sorting. For a return period RP the yearly maximum discharge is then estimated as $Q_{(k)}^{Max}$ where $k = 20001 - 20000 / RP$. In summary this means that for each RP an appropriate quantile of the empirical distribution of the Q^{Max} must be obtained.

In this way the discharge for the maximal retrievable return period $RP=20000$ is given by $Q_{(20000)}^{Max}$, for $RP=10000$ by $Q_{(19999)}^{Max}$, for $RP=5000$ by $Q_{(19998)}^{Max}$, etc. For such high return periods (corresponding to high quantiles of the empirical distribution) a high sensitivity will be found for the (tail of the) sample Q^{Max} . A way to reduce this sensitivity is to use a large(r) part of the sample's tail in the estimation of the quantile instead of merely a single data point. In this way the accuracy of the estimate of the $Q^{Max}(RP)$ can be improved for high return periods RP (i.e. reduction of the estimate's variance).

In the present case the Weissman procedure (Weissman, 1978) was followed for improved estimates of high quantiles. The essence of Weissman's estimator of high quantiles is a fitting of an exponential distribution to the k -largest values $Q_{(k)}^{Max}$ of the sample. This is only meaningful if the tail of the distribution is not heavier than exponential (see Boos, 1984). After the fitting the 'observed' $Q_{(k)}^{Max}$ are replaced by the corresponding fitted values. This 'smoothing' of the sample $\{Q_{(\ell)}^{Max}\}_{\ell=1}^{20000}$ is done for the high quantiles only, i.e. the $Q_{(\ell)}^{Max}$ with $\ell \geq k$. The 'low' quantiles are not affected and remain as derived straightforwardly from the empirical distribution.

Above it was mentioned that within the Weissman procedure the highest k observed quantiles can be replaced by the corresponding fitted values. More generally, and at the same time, the procedure can conveniently be used for extrapolation, and thus to find estimates of the extremes associated to return periods much longer than the maximum return period determined by the size of the observed sample.

The Weissman procedure has been applied to the annual extremes $\{Q_{(\ell)}^{Max}\}_{\ell=k}^{20000}$ of every (i,j) variation in the uncertainty matrix. The 'threshold' k was set to the value that corresponds to a return period of 250 year. With a 20,000 years length of the simulated time series this leads to $k=20001 - 80 = 19921$. On the other hand, in GRADE simulations with a reference weather series of length 50,000 years, the 'threshold' k was set to the value that corresponds to a return period of 500 year.

Below, in Figure A.3.1, the effect of a Weissman procedure is shown by a probability plot. In this figure annual maxima are plotted versus their probability on non-exceedence (actually a non-linear transformation of the quantiles). The loose blue symbols * represent the probability plot of the HBV discharge extremes at Borgharen derived from the GRADE reference simulation of the Meuse. In this reference simulation of length 20,000 year the reference synthetic rainfall series was used as model forcing (i.e. synthetic rainfall and temperature where in weather generator all observed weather data served as basis set), and the 50% HBV parameter combinations in the hydrological models. For the same simulation the red solid curve in Figure A.3.1 shows this probability plot after application of the Weissman procedure. The smoothing effect for the highest quantiles is clearly recognised. The dashed part of the red curve shows how at the same time the Weissman method was also used for extrapolation.

In the uncertainty analysis such a Weissman smoothing of the highest quantiles was (separately) performed for every combined of the variation of the model forcing and the HBV-parameters sets.

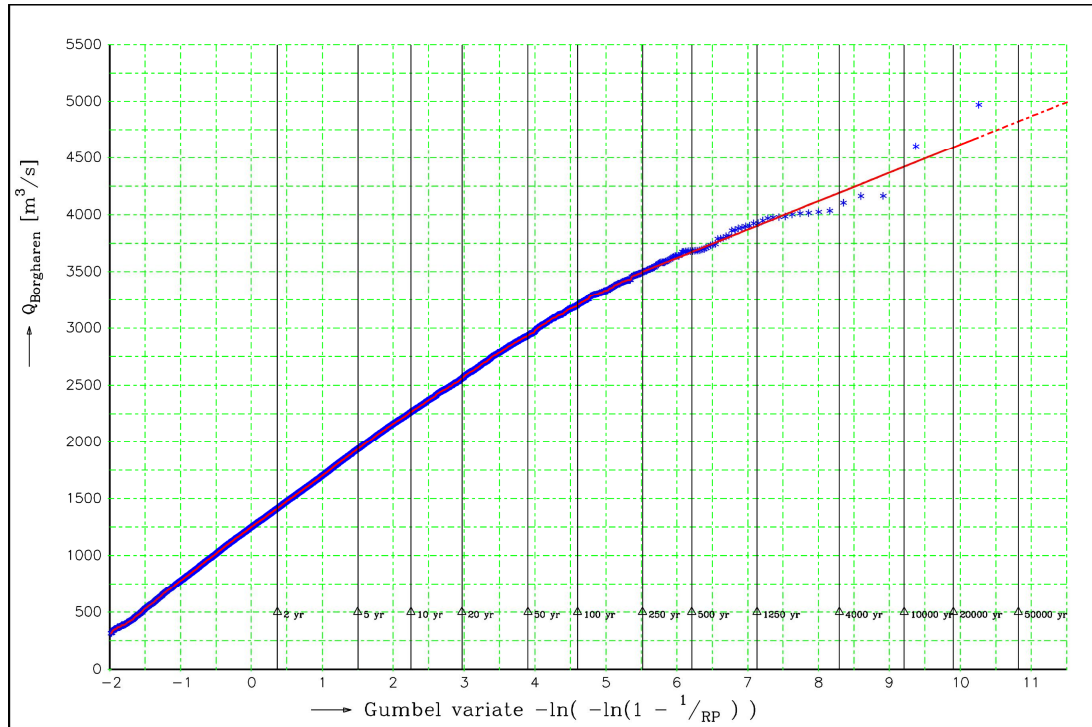


Figure A.3.1 Effect in probability plot of Weissman smoothing of high quantiles. Here applied to GRADE computed discharge extremes of the Meuse at Borgharen, with the reference synthetic rainfall and temperature series, and with the 50% quantile set of the HBV-parameters

A.4 Quantifying the uncertainties in the climate

For a given return period RP , and the j -th HBV-parameter combination ($1 \leq j \leq 5$), the j -th column in the Uncertainty Matrix of Table A.1.1 provides a set of N estimates $\{Q_{RP}(i, j)\}_{i=1}^N$ for the associated annual maximum discharge $Q(RP)$. For the Rhine the sample size $N=11$ and for the Meuse $N=24$.

For ease of notation the subscript RP is omitted in the expression $\{Q_{RP}(i, j)\}_{i=1}^N$ and also in other formulas in the remainder of this section the dependency on the return period is not always explicitly indicated.

From the $\{Q(i, j)\}_{i=1}^N$ an estimate for the mean value $m_{WG}(j)$ of $Q(RP)$ is derived, together with a measure for the uncertainty. This uncertainty in $Q(RP)$ is then due to the uncertainty in the weather climate, i.e. the synthetic temperature and rainfall time series. The procedure to obtain this column wise combined estimate of $Q(RP)$ and its uncertainty is described below.

As a matter of the construction of the synthetic rainfall series each of the N constructed synthetic rainfall series are equally likely. As a result a uniform distribution can be assumed for the $\{Q(i, j)\}_{i=1}^N$. Therefore the standard arithmetic mean provides a best estimate for (the expected value of) the discharge maximum $Q(RP)$:

$$m_{wG}(j) = \frac{1}{N} \sum_{i=1}^N Q(i, j) \quad (\text{A4.1})$$

For a quantitative measure of the uncertainty in $Q(RP)$ the spread (or standard error) can be used. In this case the standard formula for the spread cannot be applied, however. The reason is that the N data points $\{Q(i, j)\}_{i=1}^N$ are not mutually independent. This is a consequence from the Jackknife recipe that was followed in the selection of the N basis sets from the total sample of historic weather data. The N resamples of the historic data set that serve as basis sets for the weather generator have a large overlap in time. These dependencies must appropriately be taken into account when computing statistics. In particular this holds for the computation of the standard error in the mean given by Equation A4.1. In fact, for the presently used Jackknife delete block resampling it can be shown that this standard error is given by:

$$s_{wG}(j) = \sqrt{\frac{N-1}{N} \cdot \sum_{i=1}^N (Q(i, j) - m_{wG}(j))^2} \quad (\text{A4.2})$$

Note that in this way the standard error is about \sqrt{N} times as large as the value that would be found with the standard formula for mutually independent data points $\{Q(i, j)\}_{i=1}^N$.

For the derivation of Equation A4.2, and/or more generally the theoretical background, algorithms, and statistical inference in Jackknife (delete block) resampling one is referred to Efron and Tibshirani (1993) and Davison and Hinkley (1992).

More generally the uncertainty in the discharge $Q(RP)$ due to the weather climate can be represented by means of a probability distribution $\varphi(\cdot)$. The mean of this distribution is already obtained through Equation A4.1. Moreover, the standard error in the mean, as prescribed by Equation A4.2, provides the spread of the distribution. For a statistically complete representation of $\varphi(\cdot)$ also higher order characteristics (such as moments or cumulants) of the distribution should be derived. In contrast to the mean and spread, no expression is known for the computation of these higher order characteristics from a Jackknife resample $\{Q(i, j)\}_{i=1}^N$. At the same time the present sample size N is rather small which also hampers a solid estimation of higher order moments. Therefore we can do not much better than to assume that for a given HBV-set the estimate for the discharge is normally distributed with the mean and spread provided by the Equations A4.1 and A4.2.

An "aggregation" as described above can be carried out for each of the $M=5$ columns of the Uncertainty Matrix, i.e. for each separate variation of the HBV-parameters. In the end this gives a set 5 normal distributions $\{\varphi_j(\cdot | \mu_j, \sigma_j)\}_{j=1}^M$ with mean $\mu_j := m_{wG}(j)$ and spread $\sigma_j := s_{wG}(j)$. These distributions represent the weather climate induced uncertainty in the annual maximum discharges for the given HBV parameter sets.

It must be noted that at this moment these $\varphi_j(\cdot | \mu_j, \sigma_j)$ are ‘merely’ conditional distributions. In fact, $\varphi_j(\cdot | \mu_j, \sigma_j)$ gives the distribution of the discharge under the condition of the j -th HBV parameter set.

In next sections it will be described how together with the present combination over the columns of the Uncertainty Matrix also a combination must be carried out over the rows (HBV-parameter combinations) to get the ‘total’ estimate of, and overall uncertainty in, the discharge $Q(RP)$ for a given return period RP .

A.5 Quantifying the uncertainties in the hydrological models

The uncertainty induced by the hydrological models has been represented by $M=5$ sets of HBV model parameter combinations. These combinations were selected from all behavioral parameter combinations that were found in a GLUE based calibration of the HBV-models of the various sub-basins. The five selected parameter combinations correspond to the 5, 25, 50, 75, and 95% quantiles of the set of extreme discharges that was computed for all (or a representative subset) behavioral HBV-model parameter combinations.

For a given return period RP , and also given i -th synthetically generated weather series, the estimate and uncertainty for the associated annual maximum discharge $Q(RP)$ must then be derived from $M=5$ GRADE predictions $\{Q_{RP}(i, j)\}_{j=1}^M$. These $\{Q_{RP}(i, j)\}_{j=1}^M$ correspond to the five sets of HBV-parameter combinations, and form a row in the Uncertainty Matrix.

For ease of notation the subscript RP is omitted in the expression $\{Q_{RP}(i, j)\}_{j=1}^M$ and also in other formulas in the remainder of this section the dependency on the return period is not always explicitly indicated.

As a matter of their construction the five HBV parameter sets are not equally likely and a proper probability or weight must be assigned to them. These weights are required in the combination of the uncertainties along the rows in the Uncertainty Matrix. For assigning weights $\{w_j\}_{j=1}^M$ to the five sets of HBV-parameter combinations several procedures may be feasible. In the present approach the weights were derived from the distribution of the extreme discharges that within the calibration phase were computed for all behavioral parameter combinations. This set is the same set as the one from which through a quantile selection criterion the five HBV parameter combinations were derived. To obtain a proper quantitative representation of this distribution, a large number of analytical and parameterised probability density functions $f(\cdot | \Theta)$ (uniform, Gaussian, exponential, Gumbel, Weibull, Reversed Weibull, Log-Normal, Beta, etc.) was fitted to the set of extreme discharges. The distribution $f(\cdot | \hat{\Theta})$ providing the best fit to the ‘empirical’ distribution was selected.

For each of the five non-exceedence probabilities P_j , with P_j one of $\{0.05, 0.25, 0.5, 0.75, 0.95\}$, the x_j was computed such that $F(x_j | \hat{\Theta}) = P_j$ (or equivalently: $x_j = F^{Inv}(P_j | \hat{\Theta})$). This $F(\cdot | \hat{\Theta})$ is the cumulative distribution function of the $f(\cdot | \hat{\Theta})$ introduced and described in the preceding paragraph. The weight that is then assigned to the

j -th set of HBV parameter combinations is the conditional probability $w_j = \text{Prob}[x = x_j | x = x_1 \text{ or } x = x_2 \text{ or } x = x_3 \text{ or } x = x_4 \text{ or } x = x_5]$. This then readily yields $w_j = f(x_j | \hat{\Theta}) / \sum_{j=1}^M f(x_j | \hat{\Theta})$. As a matter of the construction the normalization $\sum_j w_j = 1$ holds.

For the Rhine 5 representative parameter combinations were derived for every of the 15 major sub-basins separately. Formally the above described procedure for finding appropriate weights for these representatives must then be carried out for every sub-basin as well. In the present work the weight estimation was restricted to two major sub-basins: the Moselle and the Neckar basin. For both of these sub-basins a Reversed Weibull probability distribution provided a best fit for the set of extreme discharges. The Reversed Weibull distribution is defined by the following cumulative distribution function:

$$F(x | \Theta) = \exp\left[-\left(-\frac{x-x_0}{\sigma}\right)^\alpha\right] \quad \text{for } x \leq x_0, \text{ and}$$

$$F(x | \Theta) = 1 \quad \text{for } x > x_0$$

For an impression of the quality of the fits of this distribution to the set of extreme Moselle and Neckar discharges one is referred to the Figures A5.1 and A5.2. In these figures the empirical distribution and the identified analytical distribution are compared by means of a Quantile-Quantile plot. The position of the 5, 25, 50, 75, and 95% quantiles are indicated by the red dashed horizontal and vertical lines.

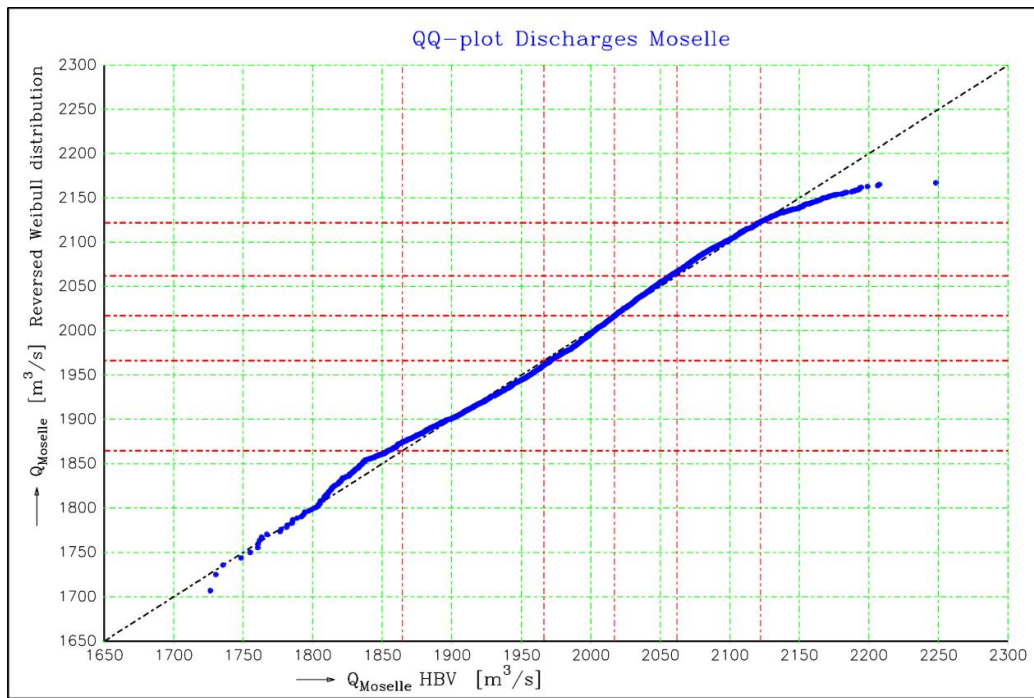


Figure A.5.1 Quantile-Quantile plot of the empirical and fitted reversed Weibull distribution of extreme discharges of the Moselle basin.

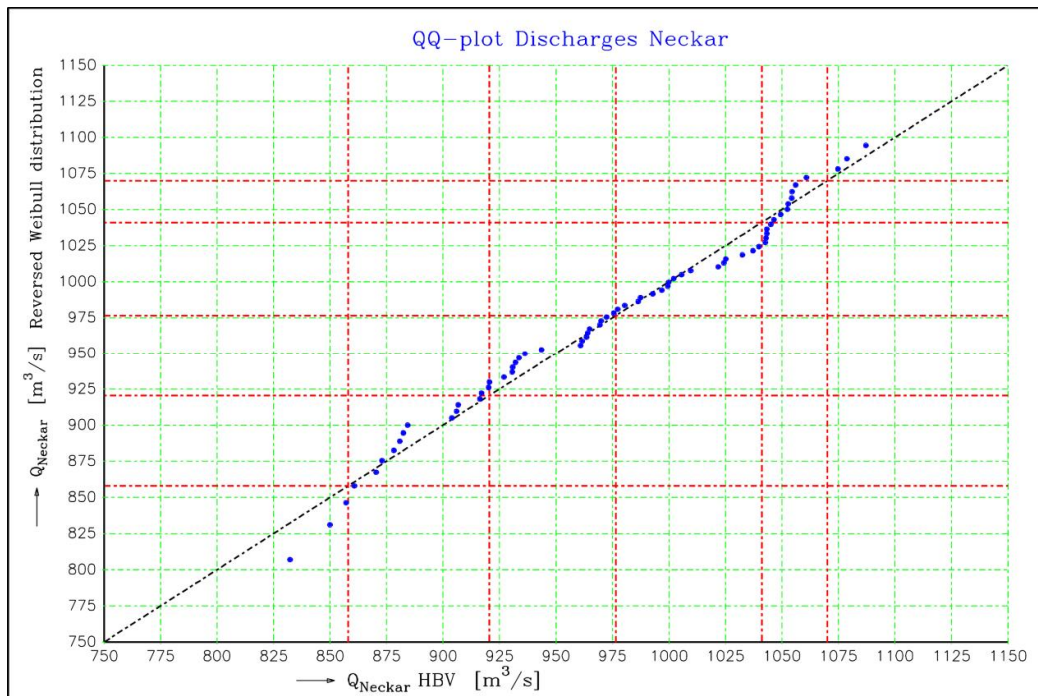


Figure A.5.2 Quantile-Quantile plot of the empirical and fitted reversed Weibull distribution of extreme discharges of the Neckar basin.

For the Moselle and the Neckar the estimates of the shape parameter α in $F(x|\Theta) = \exp\left[-\left(-\frac{x-x_0}{\sigma}\right)^\alpha\right]$ turned out to be virtually the same and amounted $\hat{\alpha} = 2.25$.

This same $\hat{\alpha}$ then yields also equal weights for the five HBV parameter combinations of the two sub-basins. NB: it is readily verified that after normalization the weights are independent of the location parameter x_0 and scale parameter σ , and only depend on the shape parameter α .

In the end this gives the following weights 0.0678, 0.221, 0.300, 0.277 and 0.134 for the 5 HBV-parameter combinations.

The so identified equal weights for the Moselle and the Neckar were assumed to hold for all the other sub-basins as well, and more generally also for the quantile based combination of the HBV-parameters over the sub-basins (see Section 2.2). The weights obtained are thus particularly applied for the discharge of the whole Rhine basin at Lobith.

On the basis of the weights $\{w_j\}_{j=1}^5$ the following expressions are readily obtained for an estimate of the discharge $Q(RP)$ and its spread:

$$m_{HBV}(i) = \sum_{j=1}^5 w_j \cdot Q(i, j) \tag{A5.1}$$

$$s_{HBV}(i) = \sqrt{\sum_{j=1}^5 w_j \cdot (Q(i, j) - m_{HBV}(i))^2} \tag{A5.2}$$

The s_{HBV} then represents the uncertainty in $Q(RP)$ due to the uncertainty in the hydrological models.

Since the weights provide a ‘complete’ (discrete) probability distribution any other statistical measure can be derived from these weights as well. In contrast to the situation in Section A4 (where we had to deal with mutual dependencies in the sample $\{Q(i, j)\}_{i=1}^N$) no further assumptions and/or approximations have now to be applied.

It must yet be recapitulated that mean and spread presented in Equations A5.1 and A5.2 are conditional with respect to the i -th synthetic weather series.

A.6 Combination of the uncertainties in the climate and hydrological models

The combinations along the columns and rows of the Uncertainty Matrix as described in the two preceding sections must now be combined to obtain an overall estimate of, and overall uncertainty in a discharge extreme $Q(RP)$.

The final result in Section A.4 for the uncertainty in $Q(RP)$ induced by the (uncertainties in the) weather climate consists of five Gaussian distribution functions $\varphi_j(\cdot | \mu_j, \sigma_j)$. Next, in Section A.5, probabilities (actually normalised weights $\{w_j\}_{j=1}^5$) have been derived for the five sets of HBV model parameter combinations that reflect the uncertainty in the hydrological models.

Strictly speaking there may be a correlation between the uncertainties in the weather variables on one hand and the HBV-parameters on the other. The reason is that the estimates and uncertainties of the HBV parameters are based on the data (and particularly the historic weather data) used within the calibration of the HBV-models. In this calibration uncertainties in the data have hardly or not been considered and neither an assessment of how variations in the weather data affect the estimates of, and uncertainties in, the HBV-parameters. This is not further investigated and presently it is assumed that the uncertainties in the model forcing and in the HBV models are fully independent.

Under this assumption of independent weather variables and HBV-parameters, and using standard formulas for conditional probabilities, it can easily be verified that a combination over the rows and next the columns of the Uncertainty Matrix yields the following expression for the probability density function $f(\cdot)$ for a discharge extreme $Q(RP)$:

$$f(Q) = \sum_{j=1}^M w_j \cdot \varphi_j(Q | \mu_j, \sigma_j) \quad (A6.1)$$

From this distribution $f(\cdot)$ the mean (m) can be computed as the ‘overall’ combined estimate for $Q(RP)$. With $\mu_j := m_{WG}(j)$ and $\sigma_j := s_{WG}(j)$ (see Equations A4.1 and A4.2) this gives the following result:

$$m = \sum_{j=1}^5 w_j \cdot m_{WG}(j) \quad (A6.2)$$

The ‘final’ estimate for $Q(RP)$ is thus a weighted average of the column wise means that were found in the combination of the weather climate variations. Since the weights are non-negative and sum up to 1, we particularly have that:

$$\text{Min}\left(\{m_{WG}(j)\}_{j=1}^M\right) \leq m \leq \text{Max}\left(\{m_{WG}(j)\}_{j=1}^M\right) \quad (\text{A6.3})$$

The overall mean m is thus bounded by the minimum and maximum of the marginal means within the combination of the uncertainties in the climate variables.

From Equation A6.1 also the spread of the distribution $f(\cdot)$ can be computed as a measure for the uncertainty in the estimate for the discharge. In fact, the variance is given by

$$\begin{aligned} \int Q^2 \cdot f(Q) \cdot dQ - \left(\int Q \cdot f(Q) \cdot dQ\right)^2 &= \sum_{j=1}^M w_j \cdot (\mu_j^2 + \sigma_j^2) - \left(\sum_{j=1}^M w_j \cdot \mu_j\right)^2 = \\ &= \left(\sum_{j=1}^M w_j \cdot \mu_j^2 - \left(\sum_{j=1}^M w_j \cdot \mu_j\right)^2\right) + \sum_{j=1}^M w_j \cdot \sigma_j^2 = \\ &= \sum_{j=1}^M w_j \cdot \left(\mu_j - \sum_{j'=1}^M w_{j'} \cdot \mu_{j'}\right)^2 + \sum_{j=1}^M w_j \cdot \sigma_j^2 \end{aligned}$$

In the end this then provides the following expression for the standard deviation s :

$$s = \sqrt{\sum_{j=1}^5 w_j \cdot [m_{WG}(j) - m]^2 + \sum_{j=1}^5 w_j \cdot s_{WG}^2(j)} \quad (\text{A6.4})$$

In this way the overall variance s^2 in $Q(RP)$ is a superposition of a variance in the ‘marginal’ means $\{m_{WG}(j)\}_{j=1}^5$ on one hand, and a weighted mean of the marginal variances $\{s_{WG}^2(j)\}_{j=1}^5$ on the other.

In the uncertainty matrices that are presented in Chapter 4 (Rhine) and Chapter 5 (Meuse) the means (m_{WG} and m_{HBV}) and spreads (s_{WG} and s_{HBV}) found for the two marginal distributions are also listed. Similarly the final estimate or $Q(RP)$ (m as computed with Equation A6.2) and its spread (s as computed with Equation A6.4) are shown in the tables.

From the mean and the spread of $Q(RP)$ a symmetric confidence interval of the form $m \pm z_\gamma \cdot s$ can be computed. For a $\gamma=95\%$ confidence level z_γ will be approximately 1.96. In theory this (approximation for a 95%) symmetric confidence interval is only valid if $Q(RP)$ is normally distributed. For the most extreme floods this may not be true and even the assumption of a symmetric distribution is doubtful. This will particularly be the case when the river’s peak discharges are affected by flooding of floodplains and dike overflows. For such flow conditions the distribution of $Q(RP)$ may be highly skew and become bounded from above. Skew confidence intervals then provide a much better representation of the uncertainty. To obtain reasonably accurate estimates for the lower and upper bound of a skew 95% (or 99%, or even higher) confidence levels the sample size must be sufficiently

large, however. In the present case the sample size of empirical distribution of the $Q(RP)$ (i.e. the dimension of the Uncertainty Matrix, and thus the number of available GRADE estimates $\{Q_{RP}(i, j)\}$) tends to be too small to satisfy this demand. For this reason we presently restrict to symmetric confidence intervals only. More 'dense' evaluations of the uncertainty matrix (GRADE computations for a much larger number of variations of the model forcing and/or the HBV-parameter combination), and/or additional theoretical assessments how to take skewness more thoroughly into account must be mentioned as important future topics for improvement of the present uncertainty analysis.

B Regression of HBV and SOBEK estimates of extreme Rhine discharges at Lobith

In Section 4.2 and Section A.2 of Appendix A it has been argued that to save computation time SOBEK runs were ‘merely’ carried out for the reference synthetic weather series combined with the 50% HBV parameter set. These GRADE reference simulations were of length 50,000 years. From the results of the HBV and SOBEK simulations the set of corresponding annual extreme discharges $\left\{ \left(Q_k^{Max, HBV}, Q_k^{Max, SOBEK} \right) \right\}_{k=1}^{50000}$ was selected. From this set a parameterized formula $f(\cdot | \Theta)$ is identified to “predict” the $Q^{Max, SOBEK}$ from the $Q^{Max, HBV}$. The calibrated function $f(\cdot | \hat{\Theta})$ can then be applied to all entries of an HBV uncertainty matrix to obtain a suitable approximation of this matrix for the case it would have been generated with SOBEK.

Such a formula $f(\cdot | \Theta)$ was derived in twofold: first for the case that the $Q^{Max, SOBEK}$ were computed with SOBEK without facilities for flooding, and secondly for the $Q^{Max, SOBEK}$ according to the SOBEK model in which effects of flooding are included. In this section the so identified functions $f(\cdot | \Theta)$ are presented below.

B.1 SOBEK without flooding

Figure B.1.1 shows a scatterplot (blue symbols *) of the mutually corresponding Lobith annual discharge extremes $\left\{ \left(Q_k^{Max, HBV}, Q_k^{Max, SOBEK} \right) \right\}_{k=1}^{50000}$ that were found with the HBV models and the SOBEK model without flooding. As mentioned above the data points are for the GRADE simulation with the reference model forcing combined with the reference HBV parameters.

Despite significant scatter, this figure reveals a reasonably unique and monotonous relation between the HBV and SOBEK extremes. Through regression a formula has been identified to ‘translate’ HBV extremes to a corresponding SOBEK value. The adopted regression formula for $f : Q^{Max, HBV} \rightarrow Q^{Max, SOBEK}$ is of the form:

$$f(Q | \vec{\alpha}) = \alpha_1 + \alpha_2 \cdot (Q - \alpha_3) + \alpha_4 \cdot \ln \left(1 + \exp \left(\alpha_5 \cdot (Q - \alpha_3) \right) \right) \quad (\text{B.1.1})$$

For the parameters $\vec{\alpha}$ in this formula the following estimates were found: $\hat{\alpha}_1 = 14342 \text{ m}^3/\text{s}$, $\hat{\alpha}_2 = 0.915$, $\hat{\alpha}_3 = 15203 \text{ m}^3/\text{s}$, $\hat{\alpha}_4 = 466 \text{ m}^3/\text{s}$, and $\hat{\alpha}_5 = 4.37 \cdot 10^{-4} \text{ s}/\text{m}^3$. The quality of this regression can be verified from the red curve in Figure B.1.1. This quality is by all means reasonable for the whole domain spanned by the data.

Note that shape of the regression curve is slightly curved but remains close to linear (and also close to identity) over the whole domain of extreme discharges. For the highest discharges (higher than 16,000 m^3/s , say) the slope of the regression curve tends to increase and become slightly larger than one.

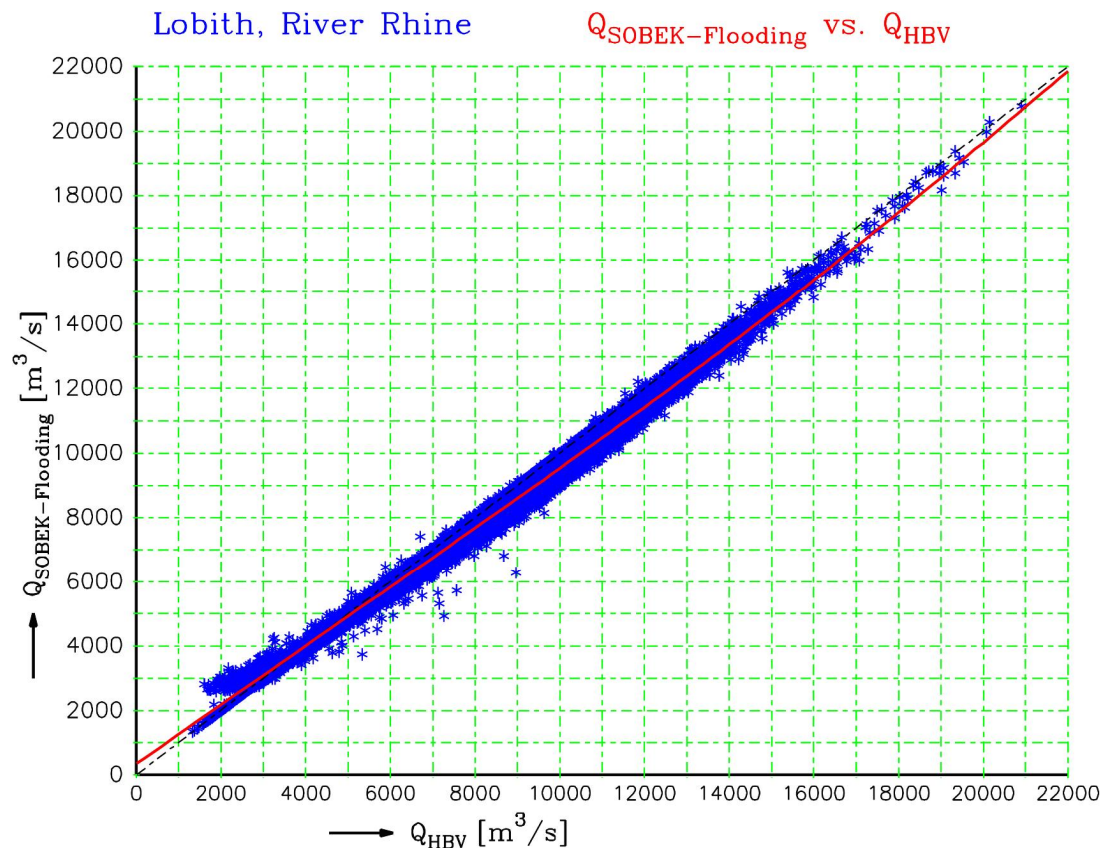


Figure B.1.1 Scatterplot of SOBEK based annual discharge extremes at Lobith versus the ones according to HBV. In this case for the SOBEK model without flooding

B.2 SOBEK with flooding

Figure B.2.1 shows a scatterplot (blue symbols *) of the mutually corresponding Lobith annual discharge extremes $\left\{ \left(Q_k^{Max, HBV}, Q_k^{Max, SOBEK} \right) \right\}_{k=1}^{50000}$ that were found with the HBV model and the SOBEK model *with flooding*. The data points are again for a GRADE simulation of length 50,000 years with the reference model forcing combined with the reference HBV parameters.

The same regression formula was applied as before for the modelling of the relation of the HBV and SOBEK extremes: see Equation B.1. In this case the following estimates were found for the parameters $\hat{\alpha}$ in the formula: $\hat{\alpha}_1 = 13754 \text{ m}^3/\text{s}$, $\hat{\alpha}_2 = 0.2611$, $\hat{\alpha}_3 = 14634 \text{ m}^3/\text{s}$, $\hat{\alpha}_4 = -675.1 \text{ m}^3/\text{s}$, and $\hat{\alpha}_5 = -9.71 \cdot 10^{-4} \text{ s}/\text{m}^3$.

The quality of this regression can be verified from the red curve in Figure B.2.1. This quality compares well to the one where flooding was ignored. Effects of flooding become notable as soon as the Lobith discharge is greater than about 12,000 m^3/s . For larger values (actually higher return periods than about 50 year) the Lobith discharge still increases, and in a linear way, but with a slope that is significantly less than on the left hand side. The slope in the SOBEK-HBV curve is approximately 0.27 for discharges greater than 16,000 m^3/s .

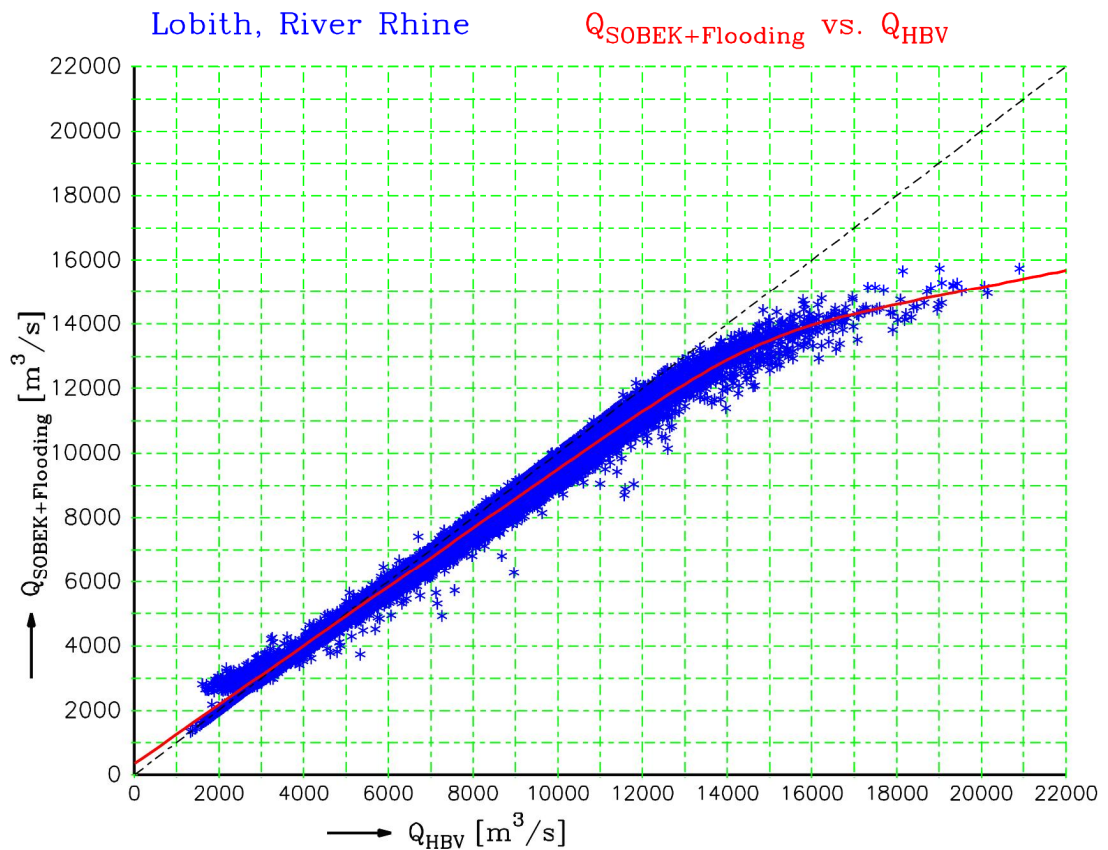


Figure B.2.1 Scatterplot of SOBEK based annual discharge extremes at Lobith versus the ones according to HBV. In this case for a SOBEK model with modelling of flooding included

B.3 Comparison of HBV and SOBEK ± Flooding

The regression curves shown in Figures B.1.1 and B.2.1 provide a convenient comparison of the SOBEK and HBV based extreme discharges. This is illustrated by the Figures B.3.1 and B.3.2. In Figure B.3.1 the two regression curves for the conversion of HBV to SOBEK (with and without flooding, and as already shown in Figures B.1.1 and B.2.1) are displayed again, but now in one figure. In Figure B.3.2 the discharges according to SOBEK with flooding is plotted versus the discharges of the corresponding SOBEK-model without flooding. From these figures it can be readily verified for which discharges effects of flooding and overflows become notable. Figure B.3.2 particularly clarifies the amount of flooding induced reduction of the Lobith discharges.

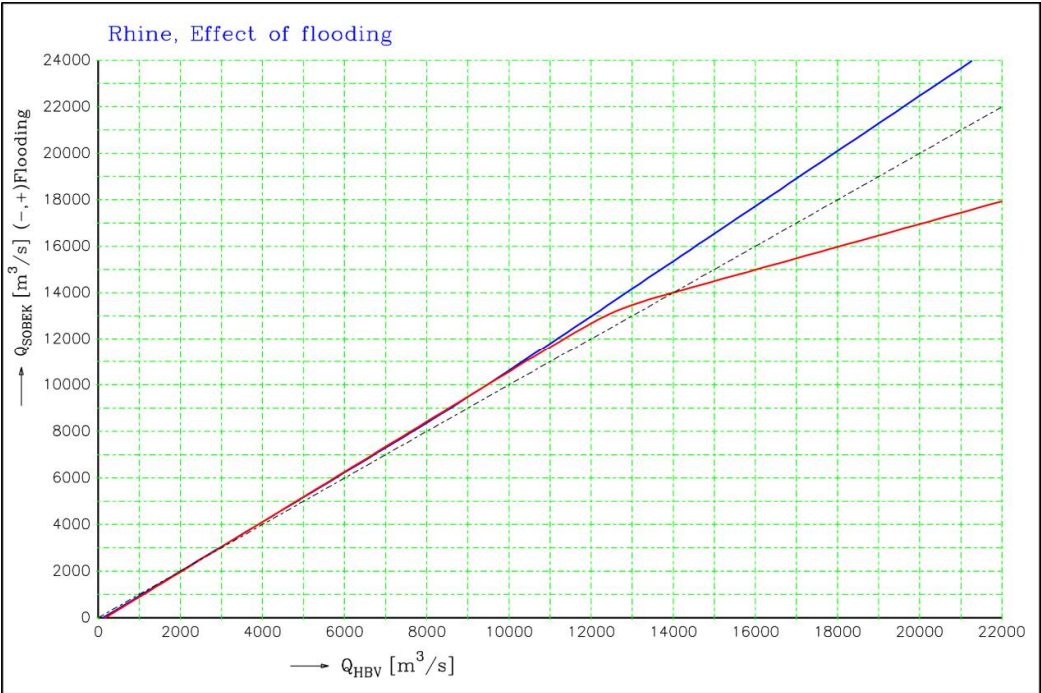


Figure B.3.1 Relation of the Lobith discharges according to HBV and SOBEK. In blue for the SOBEK model without flooding, and in red for the SOBEK model where flooding is taken into account

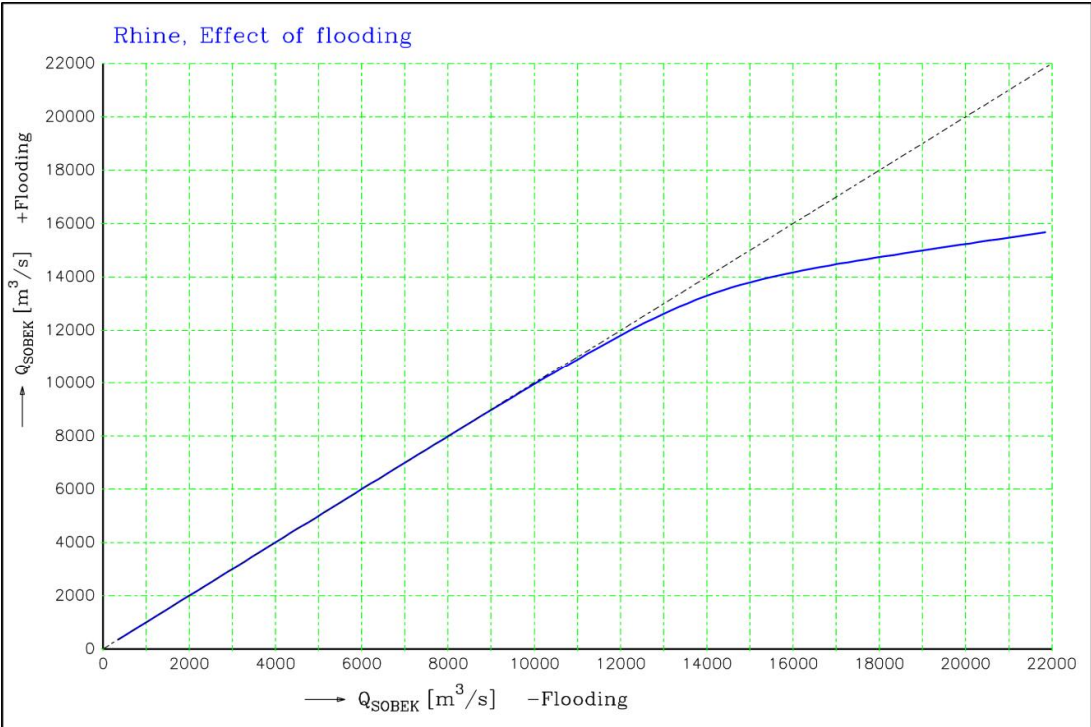


Figure B.3.2 Relation of the Lobith discharges according to SOBEK, with and without modelling the effects of flooding

C Regression of HBV and SOBEK estimates of extreme discharges of the Meuse at Borgharen

Figure C.1 shows a scatterplot (blue symbols *) of the mutually corresponding Borgharen annual discharge extremes $\left\{ \left(Q_k^{Max, HBV}, Q_k^{Max, SOBEK} \right) \right\}_{k=1}^{50000}$ that were found with the HBV model and the SOBEK model (no flooding). The data points are for a GRADE simulation of the Meuse for a time period of 50,000 years with the reference model forcing combined with the reference HBV parameters.

The same regression formula was used as for the Rhine (see Equation B.1.1) to “predict” the $Q_k^{Max, SOBEK}$ from the $Q_k^{Max, HBV}$. In the uncertainty analysis of Chapter 5 the so calibrated function $f(\cdot | \hat{\Theta})$ was used to translate all entries of the HBV uncertainty matrix into a suitable approximation of this matrix that would have been found with SOBEK.

For the parameters in the regression model the following estimates were identified: $\hat{\alpha}_1 = 792.4 \text{ m}^3/\text{s}$, $\hat{\alpha}_2 = 1.285$, $\hat{\alpha}_3 = -806.6 \text{ m}^3/\text{s}$, $\hat{\alpha}_4 = -2409 \text{ m}^3/\text{s}$, and $\hat{\alpha}_5 = 1.81 \cdot 10^{-4} \text{ s/m}^3$.

With these parameters the ‘hindcast’ of the regression formula is shown by the red curve in Figure C.1. It is readily verified that this curve hardly deviates from the diagonal plotted by the dashed black line. In fact, in a separate analysis it was found that without notable loss of quality the identity relation $Q_k^{Max, SOBEK} = Q_k^{Max, HBV}$ could have been used as well.

River Meuse at Borgharen: Q_{SOBEK} vs. Q_{HBV}

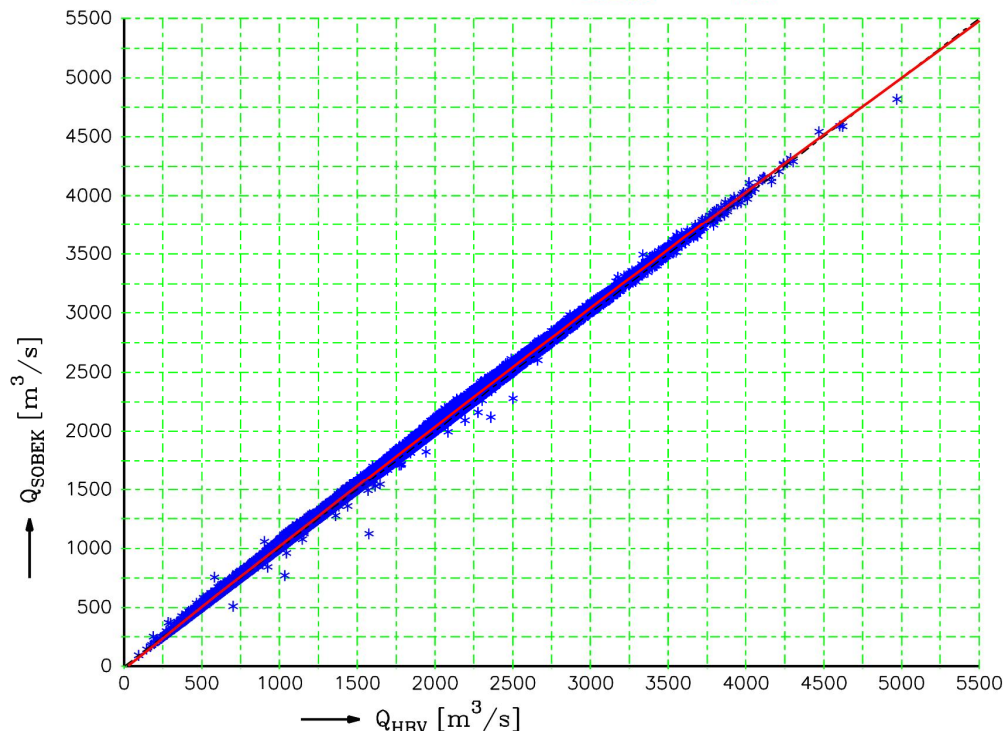


Figure C.1 Scatterplot of SOBEK based annual discharge extremes for the Meuse at Borgharen versus the ones according to HBV. In this SOBEK model flooding is not included